Assessment of One-Way Releasable Brake Mechanisms for Lower Limb Wearable Robotic Systems

A Thesis
SUBMITTED TO THE FACULTY OF
UNIVERSITY OF MINNESOTA
BY

Emily K. Brown

IN PARTIAL FULFILLMENT OF THE REQUIREMENTS
FOR THE DEGREE OF
MASTER OF SCIENCE IN MECHANICAL ENGINEERING

William K. Durfee, Advisor

March 2023

Abstract

Lower limb wearable exoskeletons can be used for weight bearing exercise by those with a spinal cord injury to mitigate adverse effects from prolonged sitting. Some exoskeletons have joints that can lock and unlock under computer control. Three categories of releasable brake technologies were analyzed to determine the best locking joint for the University of Minnesota's Functional Electrical Stimulation Energy Storing Exoskeleton: wrap spring brakes, magnetic particle brakes, and ratchet brakes. Two types of wrap spring brakes were included: off-the-shelf and custom. Fifty Newton-meters was used for the target holding torque for the analysis. Other key requirements were size, weight, power consumption when locked, and switching time. The holding torque to weight ratio of the ratchet brake was an order of magnitude higher than the other technologies. The power required to hold a magnetic particle brake in a locked state increased with holding torque. The other brake technologies consume zero power in the locked state. The magnetic particle brake was determined to be the best brake because of the high holding torque to weight ratio when coupled with a transmission, and the shape and weight optimization options. The magnetic particle brake's lack of movement after stopping and quick switching times between states are advantages that differentiate the magnetic particle brake from the ratchet and wrap spring brake. Adding additional mechanisms to limit the size of a power source needed and minimize weight of the system should be explored further.

Table of Contents

List of Tables

List of Figures

Chapter 1. Introduction

1.1 Background

Lower limb wearable robotic systems are mechanical devices designed based on the shape and function of the human body and can be worn by the operator, with segments and joints corresponding to those of the person it is coupled with. Wearable robots can integrate the cognitive ability of human beings with a robotic device to assist the users to accomplish their desired activities. The use of wearable robots is widespread and includes therapeutic applications and assistive purposes. One such type of lower limb wearable robotic systems are exoskeletons. Exoskeletons are mechanical systems designed to assist and augment the performance of the wearer's body through energy exchange with the environment. Functional electrical stimulation (FES) lower limb exoskeletons send low-level electrical impulses to nerves, which then actuate the muscles required for walking [1]. Hybrid lower limb exoskeletons combine the benefits of FES with supplemental energy storage components or power inputs to assist in proper execution of the gait cycle [2].

The Functional Electrical Stimulation Energy Storing Orthosis (FES-ESO) is an example of a developed exoskeleton that combines the simplicity of a passive exoskeleton with functional electrical stimulation of the quadriceps muscles, enabling the user to stand and walk using their own muscles [3]. In devices where the wearer employs their own muscles, it is advantageous for the hip and knee joints under the controller to lock and unlock to prevent user fatigue. A locking mechanism of the hip and knee joints holds the joints at any angle in the joint's range of motion and is important to conserve quadriceps energy from being released at improper times during gait. The locking mechanism must only allow rotation in one direction when locked with opposing rotation locked to continuously provide the necessary holding torque against gravity to prevent collapse. To complete the gait cycle, the hip joint must be able to be locked in both directions while only one direction needs to be locked for the knee joint. Thus, a releasable brake mechanism is needed for use in the hip and knee joints of an exoskeleton of this nature.

One application for a lower limb wearable robotic system is to provide assistance for those with spinal cord injuries (SCI). There are an average of 17,730 new cases of spinal cord injuries in the United States each year [4]. Loss of function in the lower body due to SCI results in mobility limitations. A wheelchair is often used for mobility, but prolonged sitting can lead to pressure sores, muscle cramps, muscular atrophy and less efficient blood flow, resulting in the accumulation of fatty acids and an increased risk of diabetes [5]. Weight bearing exercise is therefore recommended to mitigate these adverse effects. The adverse effects are mitigated further through the functional electrical stimulation aspect of lower limb exoskeletons which actuates the muscles required for walking.

1.2 Previous Art

Several lower limb wearable robotic systems that use a variety of different joint mechanisms exist commercially or are under development in academic research labs. Assistive technologies being developed can be classified in these categories: passive orthoses, powered exoskeletons for walking, functional electrical stimulation (FES) walking, and hybrid FES systems.

1.2.1 Passive Orthoses

Passive orthoses are externally applied devices used to modify the structural and functional characteristics of the neuromuscular and skeletal system. Lower-limb orthoses are classified as knee-ankle-foot orthoses (KAFOs) or hip-knee-ankle-foot orthoses (HKAFOs). If an orthoses extends across the hip joint and connects to a pelvic band or lumbar or thoracic spinal support, then it is classified as a HKAFO. If the orthoses encompasses only the knee and ankle joint and at least part of the foot then it is a KAFO. These orthoses aid in walking by either locking the joints in stance phase or by coupling movement of different joints. There is no external energy input, so the use of walking aids and upper body use is required.

The ParaWalker is an example of a hip-guidance orthosis that consists of bilateral KAFOs linked by low-friction ball bearing, free-moving hip joints [6, 7, 8]. This was found to be more efficient for walking compared to locked long leg braces. The Vannini-Rizzoli Stabilizing Limb Orthosis (V-RSLO) is a polypropylene orthosis that is configured to the shape of the lower leg. A rigid ankle joint with an angled insole angled of plantar flexion places the center of gravity of the person anterior of the ankle joint resulting in knee hyperextension stabilizing against posterior knee ligaments [9]. Locked KAFOs such as these provide good stance control but do not allow for knee flexion during the gait cycle resulting in low energy efficiency and slow gait.

The Reciprocating Gait Orthosis (RGO) with stance control has knee joints with a cam lock which provides stability during stance but free motion with flexion of the knee during swing-through [10]. A lightweight modular orthosis prefabricated KAFO made of a plastic thigh piece and an ankle-foot orthosis (AFO) was designed for children with Duchenne muscular dystrophy to extend walking ability. This system is joined at the knee with a metal joint system consisting of an automatic ring or bail lock [11].

A design for a passive hip actuation device designed to support the back while stopping and walking was proposed that included the addition of a locking mechanism to the spring joint to ensure energy conservation [12]. The design considered five hip actuation designs which included a wrap spring clutch and also considered a ratchet and pawl for the joint locking mechanism. The ratchet and pawl mechanism was not explored in this case due to their increased force requirements when unlocking under load which would require a large actuator.

The dynamic knee-brace system (DKBS) consists of a wrap spring brake that controls knee flexion [13]. Brake profile and torque capacity were identified as two areas needing further refinement were identified following preliminary system tests of a commercially available wrap spring brake. The optimization efforts reduced the profile of the brake and showed that the DKBS would properly modulate knee motion during gait. Data collection showed satisfactory performance with some difficulties in the mechanical linkage between the brake and a solenoid. It was suggested that a braking mechanism may need to be applied at both the medial and lateral pivot points in order for the DKBS to be a truly workable design.

1.2.2 Powered Exoskeletons for Walking

Powered exoskeletons for walking by people with SCI are lower-limb exoskeletons that have electric motors at the hip and knee joints, a controller to initiate and control the stepping motions, and a lithium-ion battery pack for untethered power [14]. These systems do not recruit the activation of an individual's own muscles in order for them to walk. Systems that have received FDA clearance in the U.S. include the ReWalk Robotics ReWalk, the Ekso Bionics Ekso GT, and the Parker Indego. The ReWalk Robotics ReWalk contains independently controlled bilateral hip and knee joint motors powered by rechargeable batteries and a control system that is housed in a user-worn backpack. The users control their walking through minor trunk movements and a wrist-pad controller. A tilt sensor is used to determine the trunk angle which in turn generates a prescribed hip and knee displacement resulting in a step [15]. The Ekso Bionics Ekso GT is a powered exoskeleton that enables individuals with neurological impairments to walk by supporting full body mass with motors attached at the hip and knee joints to generate steps [16]. The Parker Indego exoskeleton is a hip-knee powered exoskeleton that uses lithium-ion batteries and has an iOS pad to export data to. The bilateral hip and knee joints consist of two motors and embedded sensors and controllers [17].

Powered exoskeletons have been found to be effective in allowing users to walk [18, 19]. In a 2016 systematic review with meta-analysis, 14 studies representing 111 patients who used FDA cleared exoskeletons found that 76% of users were able to walk without assistance. These users walked an average of 98 meters on the six-minute walk test [18]. In another meta-review, the average walking speed of an individual using a powered exoskeleton was found to be 0.26 meters per second [19]. While powered exoskeletons provide opportunities for mobility-based exercise, walking exercise that is powered by the user’s muscles is desired for this application.

1.2.3 Functional Electrical Stimulation Walking

Functional electrical stimulation applies electrical stimulation to a muscle deprived of nervous system control with the objective of providing muscular contractions leading to functionally useful movement [20]. Parastep by Sigmedics Inc. in Ohio was an FES system for walking that used six channels of stimulation on the quadriceps, peroneal, and glutei surface to enable individuals with a SCI to walk with the assistance of a walker [21, 22]. Parastep was granted

FDA approval in 1994 and was developed based on previous work conducted as much as 20 years prior [23, 24]. Surface electrodes were placed on the quadriceps and gluteal muscles and the peroneal nerve and the user initiated each step while walking by using controls mounted on their walker. This system was effective for walking a short distance and had been shown to have therapeutic and psychological benefits [25, 26]. Most earlier surface FES systems are open loop control with the stimulation activated by the user.

Systems where individual muscles are directly activated using either percutaneous or implantable electrodes is another FES method. Researchers at the Cleveland VA Medical Center and Case Western Reserve University (CWRU) developed a multichannel implantable FES system that works by activating up to 48 muscles with surface, subfascial, or intramuscular electrodes [27]. Implanted systems operate on low voltage and current requirements compared to surface electrode systems. High levels of exertion and rapid muscle fatigue experienced by users as well as the inability to control joint torque in FES systems are the main challenge in these systems as well as surface systems [28].

1.2.4 Hybrid FES Systems

Hybrid FES systems combine FES with a passive exoskeleton. Some systems also combine FES with a powered exoskeleton or FES via surface spinal cord stimulation (SCS) that may then be combined with a powered exoskeleton. The FES acts as the source of energy allowing the individual to move forward. The passive exoskeleton guides joint motions to direct limb trajectories The joints of the orthosis can be locked to prevent collapse and aid in reducing muscle stimulation required thus saving power.

A hybrid system that used four channels of stimulation for walking and a self-fitting modular orthosis that used telescopic links to adjust to the user's body was designed by Popovic et al. [29]. This design used open loop control using predetermined muscles rather than closed loop control. The design was based on previous work which used a modified KAFO that placed the center of gravity anterior to the knee joint and locked the knee in hyperextension. When the center of gravity fell posterior to the knee, the quadriceps were stimulated to stabilize the knee [30, 31].

The spring brake orthosis (SBO) used elastic energy stored in springs and potential energy of limb segments. This eliminated the need for an actuator to generate hip flexion [32]. Kagaya et al. developed an orthosis with an electrical knee lock system that locked the knees in stance but allowed for swing during extension, reducing muscle fatigue and eliminating the need for stimulation during the stance and weight bearing phase [33]. The joint used within this orthosis consisted of a solenoid set on a stainless plate, and a stainless locking bar joined to the solenoid. When the knee was flexed, the knee was unlocked. When the knee was extended, the bar locked

into the groove automatically. The electrical current to the solenoid was then used to unlock the knee against gravity.

The Cleveland VA Medical Center and CWRU developed a hybrid system that used hydraulics to reciprocally couple the hips or individually lock or allow a hip to rotate in the sagittal plane. It had sixteen channels of stimulation delivered via intramuscular electrodes. The knee and ankle joints of the limb were locked during the stance phase to maximize stability, and unlocked throughout the swing phase [34, 35, 36, 37, 38]. Farris et al. described the design of a joint-coupled orthotic that used two channels of stimulation combined with a computer controlled orthosis with wafer disc brakes to aid in achieving gate [39]. All FES systems require a walking aid for balance as well as muscle strengthening exercises before individuals with SCI can fully use these systems. Even with FES systems, a high amount of energy is still required by the user to walk.

1.2.5 Human Machine and Design Lab at the University of Minnesota

The Human Machine and Design Lab at the University of Minnesota has developed several versions of a hybrid system for individuals with SCI that combines FES with a passive exoskeleton. The first version (Figure 1.1) was the controlled-brake orthosis (CBO) developed by Goldfarb [40]. The CBO is a long-leg brace that contains magnetic particle brakes at the knee and hip joints. The braking torque was continuously regulated to control swing-phase limb motion in real time and the brakes were locked during stance phase to support body weight without having to stimulate the muscles. Thus, muscle fatigue is reduced by only utilizing muscles to provide limb motion and not during stance. Preliminary testing indicated that the system functioned as intended yet some technical challenges remained including the customer acceptance of the device and the weight required to provide the needed battery power.

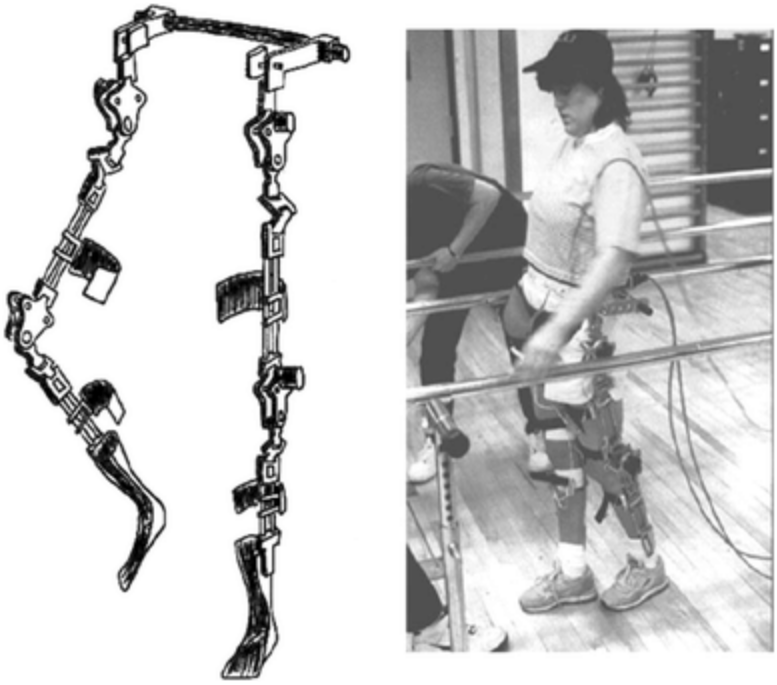

Figure 1.1. Concept rendering (left) of the CBO and the CBO shown from the side as worn by a user with SCI.

The FES-Energy Storing Exoskeleton (FES-ESE) was created to overcome some of the shortcomings of the CBO relating to using a stimulation-triggered reflex response for stepping [41, 42, 43, 44, 45, 46]. The FES-ESE (Figure 1.2) generates knee extension motion through electrical stimulation of the quadriceps while storing and releasing energy in spring elements to provide the knee and hip motion to complete the step. Computer control allows the hip and knee joint to lock and unlock in order for the exoskeleton to provide support during standing and the stance phase of walking. Several versions of the FES-ESE were studied through bench prototypes and two studies were conducted with a small number of human volunteers. The results showed that the FES-ESE concept has merit and could produce muscle-powered stepping motions through electrical stimulation of the quadriceps. The studies also showed that the FES-ESE implementations were flawed due to some design choices that were made.

Figure 1.2. Concept rendering of the FES-ESE

The FES-Energy Storing Orthosis (FES-ESO) design that is currently being developed (Figure 1.3) overcomes flaws from initial designs. High stored energy density gas springs are used for the energy storage elements. Gas springs are advantageous as they have lower cycle losses and have constant force over their stroke compared to the previously used pneumatic cylinders. Gas springs also have less hysteresis and do not deteriorate with age unlike elastomer bands which have a higher strain density. A releasable ratchet brake is used to lock and unlock the hip and knee joint rather than a magnetic particle brake. A ratchet is locked when no power is applied which is advantageous for system safety. This is not the case for magnetic particle brakes which were used in the original CBO. The ratchet does not have any take-up rotation when a reverse load is applied such as the case for wrap spring brakes that were used in several previous versions of the device. With the wrap spring brakes, take-up rotation caused the knee joint to gradually move into the flexed state over time. The FES-ESO also considered body attachment and donning and doffing from the beginning to allow for proper support of the body and an easier donning process. The weight of the exoskeleton has been reduced to 10 kilograms which is below the weight of any existing commercial power exoskeletons. A physical prototype of this version is currently being constructed to conduct performance testing and demonstrate technical feasibility [3].

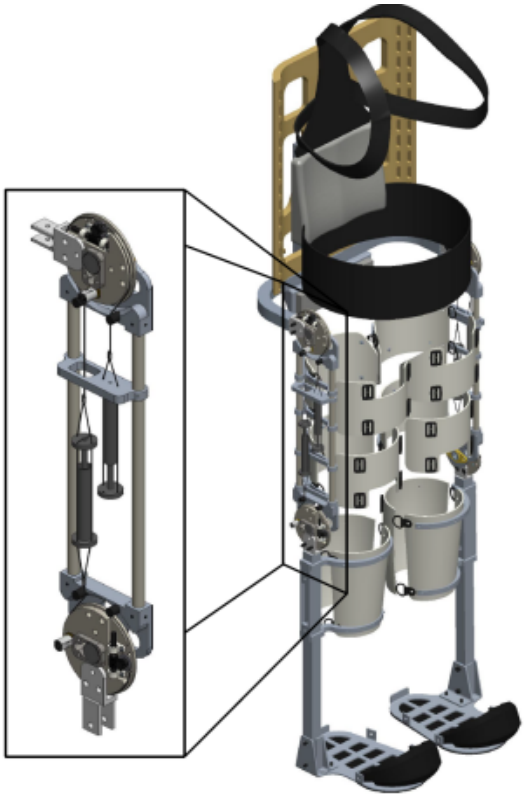

Figure 1.3. Concept rendering of the current version of the FES-ESO.

The desired gait motion is a critical component in the development of a lower limb wearable exoskeleton. The synthetic gait cycle shown (Figure 1.4) begins with the hip and knee joints flexed for the right leg (red) and extended for the left leg (green), which begins in the stance phase.

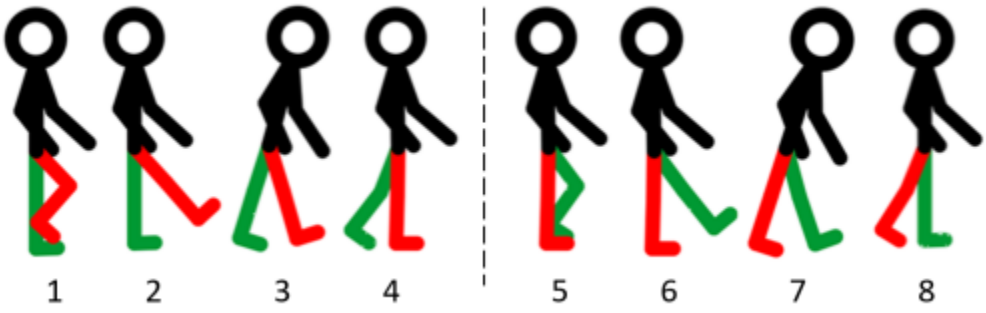

Figure 1.4. The Synthetic Gait Cycle: Steps 1-4 show the swing phase of the right leg, steps 5-8 show the swing phase of the left leg.

In the case of an exoskeleton and specifically the most recent iteration of the FES-ESO. The right knee joint in the flexed position is unlocked in the direction of extension and the quadriceps muscle ground is stimulated to promote knee extension. The stimulation of the quadriceps creates excess energy and gas springs that are tied to the hip and knee joints store a portion of this excess energy. The user then employs gravity to fall forward onto the now extended right leg, which enters the stance phase and supports the left leg as it enters flexion. At this point, the right hip joint is unlocked in the direction of extension. The hip joint is extended as the individual works to upright their torso by pushing their hands against a supportive rail. Finally, in the swing phase both the right knee and right hip joints are unlocked in the flexion direction which allows for the energy stored in the gas springs to release and actuate hip and knee joint flexion. As a result, the leg returns to the neutral position where the process is repeated for the left leg.

1.3 Study Objective

The purpose of this study was to develop analytical models and experiments to contrast the key mechanical properties of three releasable brakes to determine the best locking joint for the University of Minnesota HMDL FES-ESO system.

1.4 Design Factors For Joint Brakes

There were three major design factors that were selected to be analyzed in each of the selected one-way releasable brakes. First, the amount of external torque that the stationary but energized brakes can withstand while maintaining position was an important metric to consider when selecting a brake for a lower body wearable robotic system. The hip and knee joints must be able to withstand the weight of the user without failing. Second, the holding torque per weight of the brake was analyzed as it is important for the brake to not be heavy to prevent the overall device being too heavy which could lead to the user's muscles fatiguing. Third, the power that is required to hold the brake in the locked state was considered. The amount of power that is required is correlated to the total weight of the system because higher power means a heavier battery.

Other design factors that were considered as part of a case study of the current iteration of the FES-ESO include the volume and shape of the brakes which may influence which brake is selected based on which volume or shape would provide a more ergonomic fit. The switching time between the on and off states was also analyzed. If it takes a long time to switch between states, then the length of time for a cycle will be extended. The residual torque and damping characteristic in the released state was also examined to help determine if sagging of the joint will occur. How far the brake travels after it is locked was also considered. If the brake travels back further after each time it is locked, then the device and subsequently the user will start to sag.

1.5 Candidate Brake Technologies

One-way releasable brakes provide unidirectional rotation while locking in the other direction and have the capability to be released thus also providing unidirectional rotation in the opposite direction. Two-way releasable brakes provide bidirectional rotation and have the capability to be released. There is a difference between a brake and a clutch. A clutch is a device that provides energy transfer between two rotating shafts while a brake locks a shaft to ground which is the case for the brakes used in a lower limb wearable robotic system application. Of the technologies that are described in the previous art, wrap spring brakes, magnetic particle brakes, and ratchet brakes are the three brakes that were chosen to be explored.

1.5.1 Wrap Spring Brake

A wrap spring brake (WSB) (Figure 1.5) consists of a close-wound helical spring used to connect and transmit torque across an input hub with an output hub and control the locking and unlocking of the two. The spring is sized so that its inner diameter is smaller than the outer diameter of the hubs which generates a tight friction contact.

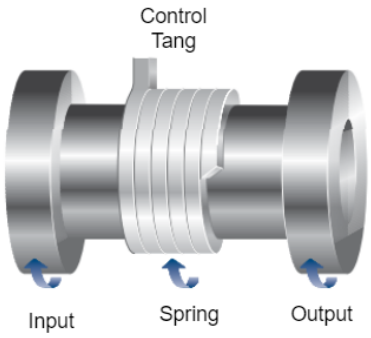

Figure 1.5. Typical components of a wrap spring brake

Torque is transmitted when the relative rotation of the input and output hubs cause the spring to wrap down on both of the hubs and apply a normal force. If the spring is unwound by the rotation of the input hub, the torque transmitted to the output hub is minimized. If the spring is wound by the rotation of the input hub, the torque transmitted to the output hub is maximized. The torque in the first coil is amplified exponentially across each successive coil due to frictional forces developed during the rotation. Adding a control tang enables the spring to be disengaged, allowing the input hub to overrun. An actuator is used to actuate the tang causing the spring to loosen or tighten. When the control tang is deflected in the direction that unwinds the spring, free rotation is then allowed. When the actuator is off, the brake rotates in the direction that winds up the wrap spring on the hub which prevents rotation. Overrunning occurs when the relative rotation of the input and output hubs causes the spring to unwind. To allow bi-directional

rotation, the brake must be released by unwinding the spring slightly and held in this expanded position so that the spring-hub friction approaches zero. When the spring is released, the brake reverts to its torque-transmitting configuration.

Slip, or the rotation in degrees before the wrap spring brake completely locks, is an inherent characteristic of a wrap spring brake. This is due to the wrap springs' floating nature between when they are released and when friction overcomes slipping and allows the spring to wind again. Each time the joint is loaded, the spring allows some movement before it coils down on the joint and stops the motion. This means that locking the joint at an exact angle is not possible with wrap spring brakes. The total number of degrees of slip increases with the amount of torque applied. If the torque is progressively applied, slip is lesser. If the wrap spring brake is unloaded every time a higher torque is applied, then the slip will be more.

If the holding torque is exceeded, the wrap spring brake will slip. This would not result in a catastrophic failure, but would compromise the overall performance of the brake. Due to exponential dependence on the frictional coefficient, the gripping torque is sensitive to friction between the discs and the wrap spring so much so that oil on the disc can cause the brake to fail. Some wrap spring brakes are intentionally lubricated so that the friction and thus performance of the brake is consistent.

Advantages of using a wrap spring brake include the ability to provide unidirectional rotation without any extrinsic control input, silent engagement at any position, low disengagement force, even then the brake is loaded, and free bidirectional rotation when disengaged [47, 48]. A wrap spring brake can be customized to fit a particular application. Some examples of aspects that can be customized include the material of the hub, the type of actuator that is used, the diameter of the hub, the spring cross section, and number of turns of the spring. Increasing the cross-section of the spring can increase the amount of torque that the brake can withstand. The materials that the hubs and springs are made and shape of these parts can also make a difference on the overall weight of the brake and fit into the device. Increasing the spring cross section expands the surface contact for braking which increases the torque and size of the brake. Increasing the number of turns of the spring increases the force gain of the brake.

Wrap spring brakes are high holding torque to weight and high holding torque to operating energy brakes with exceptional gripping torque in the locking direction and low over-running torque in the reverse direction. Since wrap spring brakes are high torque low speed devices, they do not need a transmission in the orthosis and can be directly coupled to joints. Wrap spring brakes lock only in one direction so they are well suited for the ESO application since the braking torque is needed only in flexion.

Wrap springs have a fast unlock/lock response time because the spring can be actuated with just a small motion of the spring's control tang. Another advantage that is unique to wrap springs is that the brake can be unlocked under load with only a small force needed to move the spring tang. This means that a small brake actuation brake can be used which saves space and weight in the overall device. Because the wrap spring brake is off for the majority of the gait cycle it takes in low electrical power meaning that a large and therefore heavy power source is not needed.

The operation of a wrap spring brake can be broken down into three states. The first state is when the brake is rotating in the forward direction. When the input hub turns, the spring tightens around the output hub to apply torque and accelerate the load. This state can be described by the capstan equation. The capstan equation related the hold to load force is a flexible line such as the spring is wound around a cylinder such as the brake. Because of the interaction of frictional forces and tension, the tension on a line wrapped around the cylinder may be different on either side of the cylinder. The principle behind a capstan-type device including a wrap spring brake is that a small holding force exerted on the input hub, for example, can carry a much larger loading force on the output hub. In the capstan equation, it can be seen that the force gain of the wrap spring brake grows exponentially with the number of turns in the spring, the angle of contact and the coefficient of friction.

A mathematical model of the wrap spring brake based upon strain energy, yields the following expressions for torque transmission [49].

Torque transmission in the gripping direction is

$$T_G = EIr_2 \frac{R_2 - R_1}{R_1 R_2^2} (e^{2N\pi\mu} - 1) \tag{1}$$

Torque transmission in the overrunning direction is

$$T_O = EIr_2 \frac{R_2 - R_1}{R_1 R_2^2} (1 - e^{-2N\pi\mu}) \tag{2}$$

where E is the Young's modulus of the spring material, I is the area moment of inertia of the wrap spring, r_2 is the radius of the brake, R_1 is the radius of the neutral axis of the free wrap spring, R_2 is the radius of the neutral axis of the spring on the arbor, N is the number of active spring coils, and μ is the coefficient of friction.

The capstan equation is

$$T_{load} = T_{hold} e^{\mu\phi} \tag{3}$$

where T_{load} is the applied tension on the spring, T_{hold} is the resulting force exerted at the other side of the cylinder, μ is the coefficient of friction between the spring and the cylinder materials, and ϕ is the total angle swept by all turns of the spring measured in radians where one full turn $\phi = 2\pi$.

The second step is when the input hub is stopped or reversed, but the spring is still engaged causing the spring to unwind and release the load. The third step is when the control tang is pulled back and the spring is no longer engaged and the wrap spring is freely spinning.

1.5.2 Magnetic Particle Brake

A magnetic particle brake (MPB) relies on magnetic force between two rotating disks which is transmitted by magnetic particles to produce the brake torque. The input shaft and a cylinder form the stationary member and the output shaft and rotor comprise the rotating member. The magnetic particles are dispersed within a gap between the rotor of a DC motor and the cylinder (Figure 1.6) [50].

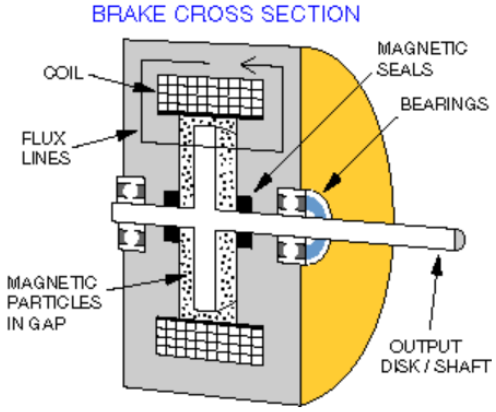

Figure 1.6. Typical components of a magnetic particle brake

When electricity is applied to the coil, a magnetic field is created causing the particles to bind together. The particles rubbing against one another causes friction which resists the relative rotation between the cylinder and rotor. As the electric current is increased, the binding of the particles becomes stronger thus increasing the braking torque that is transmitted to the rotor. Magnetic particle brakes have a wide operating torque range. The torque is independent of RPM and proportional to the magnetic field strength, and therefore to the applied D.C. input current (Figure 1.7) [51].

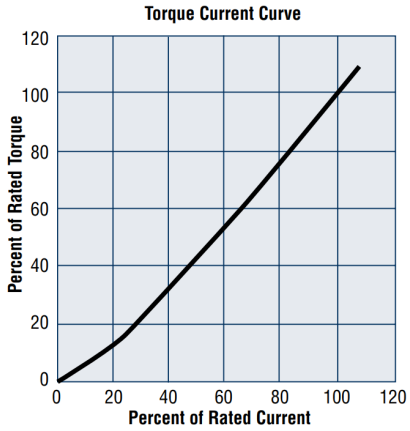

Figure 1.7. Relationship between torque and DC input current

The relationship between the torque to voltage is almost linear with the torque being able to be controlled very accurately. This makes these units suited for tension control applications as the damping is variable. They also have a fast response making them suitable for uses in high cycle frequency applications [52]. If the holding torque is exceeded, the magnetic particle brake slips.

To increase the holding torque of the brake, a transmission can be coupled to the magnetic particle brake. A transmission gear's pitch, or diametral pitch, is a number that represents the size and spacing of the teeth on an inch-sized gear. It can be estimated by taking the number of teeth plus two divided by the outer diameter of the gear. In order to mesh, the pitch of two gears must be the same. A lower pitch means the teeth are larger and farther apart. Gears with a pitch of 18 or below are often used for heavy load and low speed applications. Gears with a pitch of 20 or above have small, closely spaced teeth that run quietly at high speeds. When transmitting motion from a gear with fewer teeth to a gear with more teeth, the speed decreases while the torque increases. This can be seen through the relationship where the number of teeth times the speed of gear A equals the number of teeth times the speed of gear B. Calculating the transfer of torque is the inverse of the speed ratio or in other words, the speed multiplied by the torque of gear A equals the speed multiplied by the torque of gear B.

A smaller transmission reduces the inertia and friction, which scales with the square of the transmission ratio, that is reflected from the brake to the joint and thus uses less energy. Therefore it would be best to use a magnetic particle brake with a medium torque rating and a medium transmission rather than a magnetic particle brake with a small torque rating and a large transmission as the inertia and friction reflected from the brake to the joint would be high causing the power source required to be large and heavy.

The magnetic particle brake offers the advantage of simple control of joint torque over a bandwidth that is suitable for controlling the events involved in the human gate. It is a passive

device with no possibility of human injury resulting from unstable behavior making it well suited for uses involving human interaction. Since the brake resistance is imposed by fine ferrite particles, the engagement is smooth and quiet which is optimal for the user experience in this application.

It is a compact and lightweight means of exerting dissipative mechanical torques using an electrical control signal. When the magnetic particle brake is coupled with a transmission to provide a greater holding torque, the weight, volume and shape of the overall package presents a challenge as it is large and bulky. To help create a more ergonomic fit of the magnetic particle brake and coupled transmission for the user, the gears of the transmission can be cut down so that only the necessary section of the gear remains based on the desired range of motion. Not only will this help to minimize the volume of the joint, but it will also help to minimize the weight as the mechanical transmission is among the heaviest of the joint components. Drilling holes in the remaining part of the gear is also possible to minimize weight as long as enough material is left for the needed part strength.

1.5.3 Bi-Directional Ratchet Brake

A bi-directional ratchet brake such as the one used in a ratchet wrench is a mechanical device consisting of a gear and at least one pawl that engages the gear. Double-stacked pawls work together to alternatively engage the teeth on at least one gear as the wrench is ratcheted which is advantageous to reduce the backswing arc of the wrench. The ratchet is locked in one direction and allows rotation in the other and an actuator brake can be used to manipulate the pawls to control the direction in which the ratchet brake is allowed to rotate thus making it bi-directional. The gears can have a varying number of teeth depending on the application. The teeth are asymmetrically shaped which allows them to move past the pawl when the gear is rotated in the desired direction. The ratchet tooth count refers to how many teeth are on the drive gear which correlates to how far the user needs to move the handle to engage the next tooth. The higher the ratchet tooth count, the less the handle has to move to engage the next tooth. The arc swing, or path that the ratchet makes when ratcheting, is directly related to the number of teeth on the gear and can be calculated by

$$Arc\ Swing\ = \ 360/Number\ of\ Teeth \tag{4}$$

The ratchet provides locking that depends upon the ratchet pitch where pitch defines the angular position change between each ratchet tooth. By having a smaller pitch, the increments in joint position are smaller and a more precise joint position can be accomplished. Since the ratchet teeth are locked when under load, the joint will not slip. If the torque is exceeded, the ratchet's teeth will break causing a fully destructive failure that compromises the brake.

A ratchet's operation can be broken down into three states. The first state is when the gears are locked up against the ratchet and rotation in the one direction is not permitted, but is permitted in

the desired direction where the amplitude of its swing is fixed. When the gear is moving in the desired direction, the teeth are able to move past the pawl making a soft clicking sound. When there is no more room for the ratchet to be rotated, the second state is to rotate the ratchet back to its starting position to create more room. The third state is for the pawl to be switched using an actuator to switch the direction in which the brake is allowed to rotate to accommodate all stages of the gait cycle.

The bi-directional ratchet provides a lightweight method of locking the joint at the desired range of motion with a high holding torque that is achieved by the small ratchet pitch. A high resolution of the ratchet guides a smooth joint rotation leading to user comfort and helps simulates the gait cycle as closely as possible which is important for the user experience in this application. Since the ratchet teeth are locked when under load, the joint will not slip. There is also no take-up rotation when a reverse load is applied. Ratchets are very lightweight compared to other brakes due to the ability to use custom housing. This also minimizes the overall width of the brake which is beneficial in providing an ergonomic fit and minimally bulky design of the total system.

Chapter 2. Methods

2.1 Required Holding Torque

The highest torque value that the knee and hip joints are subjected to and thus must be able to withstand was identified. The torque acting on the hip and knee joint respectively during quiet standing with weight equally distributed between legs and phases of the gait cycle were analyzed as these were determined to be the phases in which torque acting on the joints is at a maximum. The phases of the gait cycle that were analyzed are the single-support phase, or working phases, as these are the phases in which one leg is off the ground and one leg is still in contact with the ground. This would occur for the green leg during phase one and two and for the red leg during phase five and six (Figure 1.4).

Hip and knee angles for the scenarios in which the maximum torque value is produced within the quiet standing phase and working phase and free body diagrams were used to derive hip and knee torque equations and values (Appendix A). From the free body diagram for quiet standing, the following hip and knee torque equations were developed:

$$T_{HIP} = r_{HAT}F_{HAT}sin\theta_{applied} \quad (5)$$

$$T_{KNEE} = x_{th}F_{th}sin\theta_{th} + r_{HAT}F_{HAT}sin\theta_{applied} \quad (6)$$

From the free body diagram for the working phases of the gait cycle the following hip and knee torque equations were developed:

$$T_{HIP} = r_{HAT}F_{HAT}sin\theta_{applied} + l_{th}F_{second}sin\theta_{sth} \quad (7)$$

$$T_{KNEE} = x_{th}F_{th}sin\theta_{th} + r_{HAT}F_{HAT}sin\theta_{applied} + l_{th}F_{second}sin\theta_{sth} \quad (8)$$

From these equations, the relations of the hip torque and knee torque during the quiet standing and working phase as a function of hip and knee angle were developed. A constraint that the center of mass is above the middle of the foot was used. The maximum torque value that a joint will be subjected to was then identified and used as a guideline in selecting a maximum torque requirement value to use when selecting potential brakes for a lower-limb wearable robotic system application.

For the purpose of this analysis, a torque requirement of 50 Nm was used as a guideline in selecting brakes for a lower-limb wearable robotic system application. This torque requirement value falls within a reasonable range according to calculations done and values obtained for the case of the FES-ESO (Appendix A).

2.2 Brakes Selected

Brakes that can lock and unlock were collected and ultimately selected for analysis (Table 2.1). The data sheets for each of the selected brakes show detailed information and metrics (Appendix B and C).

Table 2.1. Brakes selected for analysis

Brake Name	Type of Brake	Vendor	Model No.
WSB Commercial	Wrap Spring Brake	Warner Electric	316-17-001
WSB Custom (Hip)	Wrap Spring Brake	Reell Precision Manufacturing	N/A
WSB Custom (Knee)	Wrap Spring Brake	Reell Precision Manufacturing	N/A
MPB Commercial	Magnetic Particle Brake	Placid Industries	PLB-100
MPB w/Transmission (Hip)	Magnetic Particle Brake	Force Limited	B20SF14 (hip)
MPB w/Transmission (Knee)	Magnetic Particle Brake	Force Limited	B20SF15 (knee)
Ratchet	Bi-Directional Ratchet Brake	GearWrench	81304P

2.2.1 Wrap Spring Brake

A model 316-17-001 wrap spring brake with a static torque rating of 57 Nm from Warner Electric was analyzed using catalog data. A custom built wrap spring brake that can withstand a torque of 33 Nm and 36 Nm of torque in the knee and hip joint from a previous Energy Storing Orthosis (ESO) was analyzed using experimental data from [42] and [53].

2.2.2 Magnetic Particle Brake

A model PLB-200 magnetic particle brake from Placid Industries was analyzed using catalog data. This model has a torque range of 2 to 95 Nm. The magnetic particle brake that was used in the controlled-brake orthosis (CBO) coupled with a transmission was also analyzed using catalog data. These brakes were made by Force Limited and had custom windings. The brakes for the CBO knee and hip joint had model numbers B20SF15 and B20SF14. The knee and hip joint could resist a continuous maximum torque of 2.8 Nm and 1.8 Nm [40]. An Evoloid gear set from ASI Technologies with a 16:1 ratio was coupled with the custom magnetic particle brake, which increased the holding torque to 44.8 and 28.8 Nm.

2.2.3 Bi-Directional Ratchet Brake

A 81304P model bi-directional ratchet wrench with ½” drive and 120 XP from GEARWRENCH was selected for experimental analysis. This particular ratchet was selected due to the fine pitch or small increments in joint position and high resolution compared to most ratchet wrenches. The inner components of the ratchet head were the focus in the analysis as they would be the components used within this application.

2.3 Holding Torque per Weight

The holding torque and weight of the commercial magnetic particle brake and wrap spring brake was determined using data from the product catalogs. The holding torque of the custom made wrap spring brake was determined through published experiment data (Appendix B) [53]. The total weight of the custom made wrap spring was determined in a previous study and includes the two hubs, wrap spring, shaft collar, and washers [42]. The holding torque of the magnetic particle brake coupled with a transmission was determined through previous experimentation (Appendix B) [28]. The combined weight of the brake itself and the transmission was used as the total weight of the custom made magnetic particle brake. Five case scenarios were also analyzed for the case of magnetic particle brakes to compare the use of a large transmission and small magnetic particle brake that used 24 and 18 pitch gears, a direct drive magnetic particle brake, and a small transmission and large magnetic particle brake that used 24 and 18 pitch gears. The size of the transmission was selected to satisfy the torque requirement of 50 Nm.

The holding torque of the ratchet brake was determined using data from the product catalogs. In the published data, the manufacturer states that the ratchet meets and exceeds the ASME standards. The ASME standard for a ratchet of this type is 340 Nm [54]. As a result, this is the value that is used for the maximum holding torque for the ratchet brake. The weight of the ratchet brake was approximated by only accounting for the weight of the ratchet's internal components which was estimated to be 0.99 kg.

The holding torque per weight for all available magnetic particle brakes from Placid Industries and wrap spring brakes from Warner Electric was also collected.

2.4 Power Required to Hold Brake in Locked State

The power requirement for maintaining the lock state for wrap spring brakes and ratchet brakes is zero. The power requirement of the commercial magnetic particle brake was determined using data from the product catalogs by the manufacturers and the relation

$$P = I^2 R \tag{9}$$

The power requirement for the custom made magnetic particle brake was also determined from past experimentation (Appendix B) [28].

The torque per power for all commercially available magnetic particle brakes from a single vendor was collected and plotted. The current and resistance values for the 24 volt magnetic particle brakes were used in calculations.

Chapter 3. Results

3.1 Required Torque

The results (Table 3.1) from the full analysis conducted (Appendix A) for the torque requirement in the quiet standing scenario and the working phase scenario with both experiencing no HAT angle and a hip angle of the leg(s) on the ground of 10 degrees. For the working phase, the hip angle of the leg off the ground is 21 degrees.

Table 3.1. Maximum knee and hip torque requirement values for two scenarios based on hip angles of each leg

Scenario Name	HAT Angle	Hip Angle of Leg(s) on Ground	Hip Angle of Leg Off Ground	Hip Torque Requirement	Knee Torque Requirement
Quiet Standing	0°	10°	N/A	0 Nm	34.6 Nm
Working Phase	0°	10°	21°	7.8 Nm	78.4 Nm

3.2 Holding Torque per Weight

The plotted holding torque per weight of the seven analyzed brakes (Figure 3.1) shows the trend that the holding torque increases as the weight of the brake increases. The heaviest brake is the commercial magnetic particle brake while the lightest is the ratchet brake. The brake with the highest holding torque is the ratchet brake.

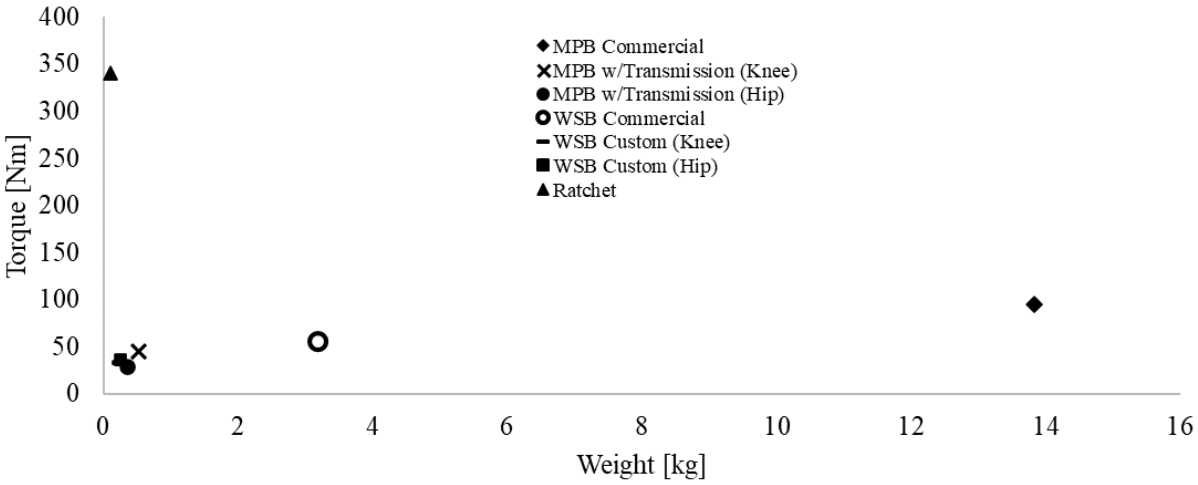

Figure 3.1. The holding torque versus weight for the brakes listed in Table 2.1. The holding torque increases with weight.

The plotted holding torque per weight of the commercially available magnetic particle brakes (Figure 3.2) shows the linear trend of the holding torque increasing as the weight of the brake increases. The dotted line represents the trendline of the data.

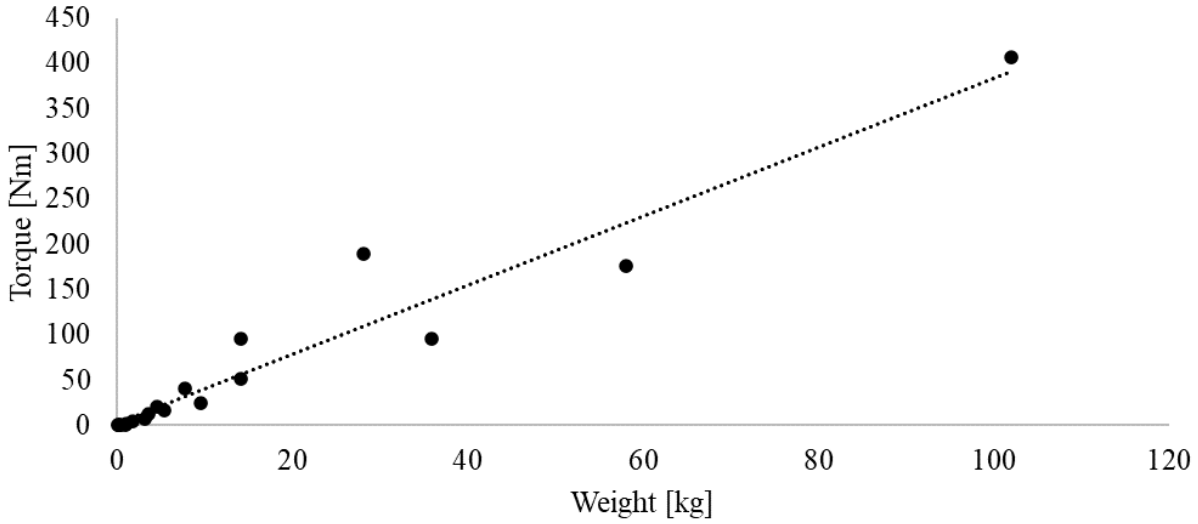

Figure 3.2. The holding torque versus weight for the commercially available magnetic particle brakes from one vendor. The dotted line represents the trendline for the plotted data. The holding torque increases with weight.

The plotted holding torque per weight of the commercially available wrap spring brakes (Figure 3.3) shows the linear trend of the holding torque increasing as the weight of the brake increases. The dotted line represents the trendline of the data.

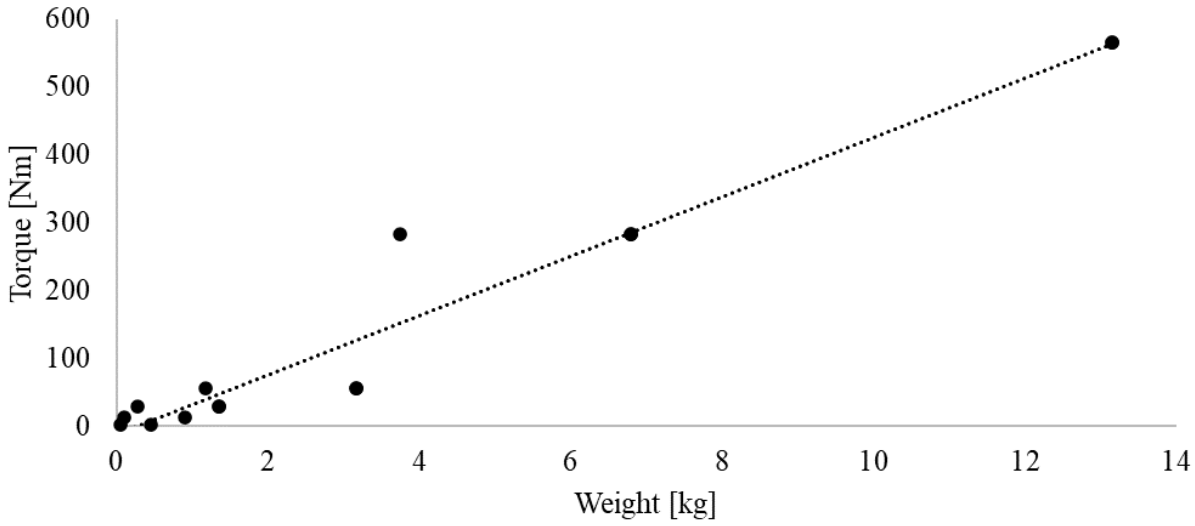

Figure 3.3. The holding torque versus weight for the commercially available wrap spring brakes from one vendor. The dotted line represents the trendline for the plotted data. The holding torque increases with weight.

The holding torque per weight was plotted for varying sizes of commercial magnetic particle brakes coupled with transmissions with gears of various pitches (Figure 3.4). The results show that a magnetic particle brake requiring a 30:1 transmission in order to meet the 50 Nm torque requirement weighed less than the magnetic particle brake requiring a 13:1 transmission in order to meet the 50 Nm torque requirement. The results also show that the brakes with the higher pitch transmissions weigh less than the brakes with the lower pitch transmissions. The highest weight of the brake packages plotted is the direct drive magnetic particle brake at over double the weight of the brakes coupled with a transmission.

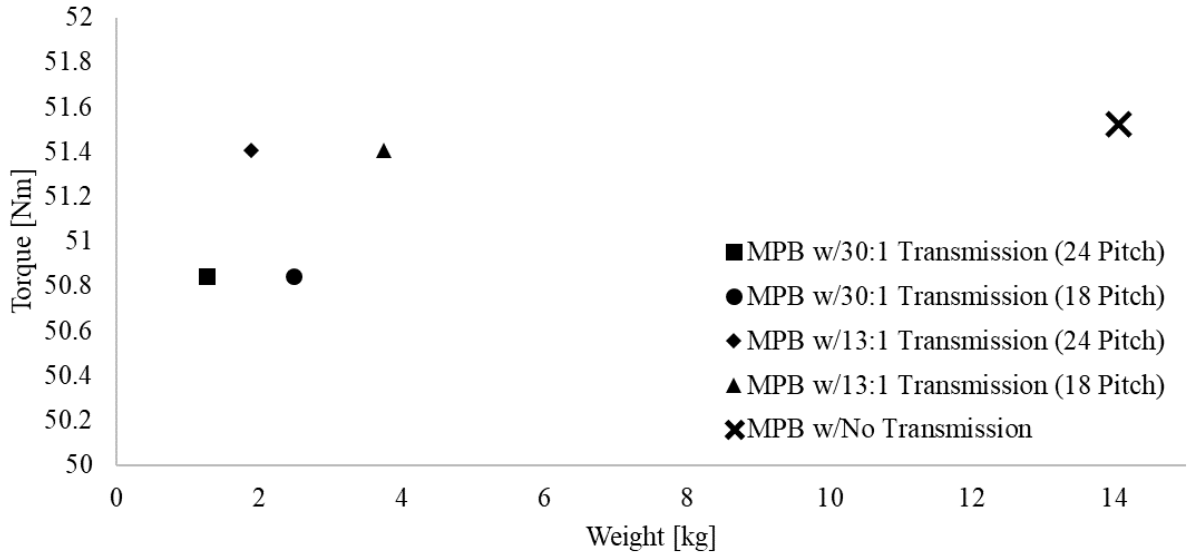

Figure 3.4. The holding torque versus weight for a magnetic particle brake that satisfies the 50 N·m torque requirement alone, a magnetic particle brake that needs a large transmission with a pitch of 24 and 18 to satisfy the torque requirement, and a magnetic particle of reasonable weight that needs a smaller transmission with a pitch of 24 and 18 to satisfy the torque requirement.

3.3 Power Required to Hold Brake in Locked State

The power as a function of holding torque for magnetic particle brakes from one vendor (Figure 3.5) shows that the power required increases as the holding torque of the brake increases. The dotted line represents the trendline for the plotted data and shows a positive relationship between power required and torque of the brake.

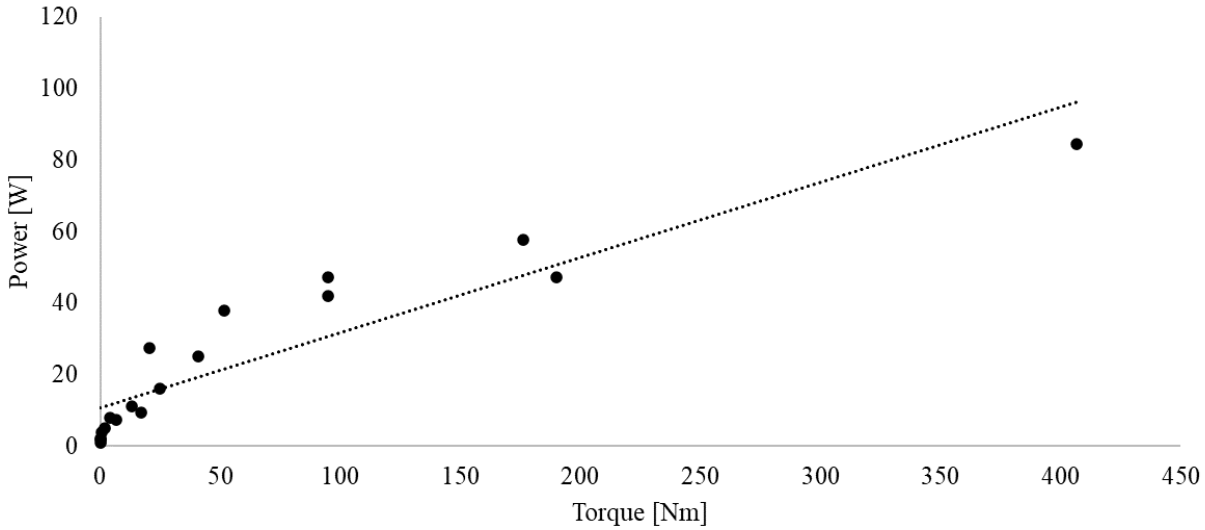

Figure 3.5. Power as a function of holding torque for magnetic particle brakes from one vendor. The dotted line represents the trendline for the plotted data. The power required increases as the holding torque increases.

Chapter 4. Discussion

4.1 Required Torque

The required holding torque is a critical metric to calculate and use when selecting a one-way releasable brake for this application to prevent brake failure. In the case of brakes with catastrophic modes of failure, it is important to add a factor of safety to the calculated torque values to ensure that failure does not occur.

The calculations were done for the hip and knee using the current version of the FES-ESO. The calculations used hip and knee posture angles and phases of the gait cycle that would produce the highest torque value to ensure that the worst case scenarios were accounted for to prevent brake failure. Anthropometrics for an individual deemed as the tallest and heaviest allowed for the system were also used within the calculations to ensure that individuals of this height and weight and all those below would be able to use the system without failure. An individual using their hands along railings to lift them up and assist in the gait cycle would reduce the torque requirement. Thus, it was assumed that an individual would not use their hands for the purposes of the calculations to account for the highest torque value possible.

In the FES-ESO maximum hip and knee torque requirements, it was found that the knee torque requirement was greater than the hip torque requirement. This is to be expected as the weight of the head and torso, HAT, as well as the thigh produces torque on the knee while just the weight of the HAT produces torque on the hip. In the case of the working phase where one leg is on the ground while the other is off the ground, additional torque is produced on the joints of the leg on the ground from the weight of the leg off the ground. This is shown in the results where the torque requirements are greater than for the case of quiet standing for the respective joints.

When the HAT is vertical, the hip joint is subject to no torque. This is not the case when the HAT is angled or leaning forward. For the purposes of this study, the case when the HAT is angled or leaning forward was not analyzed but should be considered to account for all case scenarios to ensure that the joint and system overall is designed to withstand the maximum torque requirement value.

4.2 Holding Torque per Weight

In analyzing the brakes, it was found that the holding torque increases with the weight of the brake. This aligns with the equations 1 and 2 for wrap spring brakes as a greater wrap spring brake radius, r_2, and thus weight of the wrap spring brake, leads to a larger torque transmission in the gripping and overrunning direction. A ratchet brake has the highest holding torque per weight of the three brake technologies (Figure 3.1). This makes sense as the ratchet brake is a ratchet wrench designed for high torque applications and designed to the ASME performance and safety requirements. The weight is also much lower as only the internal components of the ratchet wrench and custom housing that has been designed for weight optimization in the application of a lower limb wearable robotic systems are included in the total weight of the brake. The holding torque to weight ratio for this ratchet brake is 3434:1 (Nm:kg).

The commercial magnetic particle brake that meets the 50 Nm requirement is the heaviest brake at 13.9 kilograms. This is 7:1 Nm of holding torque per kilogram for the case of the magnetic particle brake alone. The weight is much too high to be a viable option for this application as one brake would be needed for each of the four joints on the robotic system. A magnetic particle brake can be custom made to aid in optimizing weight, but a more viable option due to the complexity of this process is selecting a transmission to pair with a magnetic particle brake to increase the holding torque of the brake.

A magnetic particle brake that has a lower holding torque is much lighter can be used in addition to a transmission to meet a higher torque requirement. This can be shown in the case of a magnetic particle brake with transmission. The holding torque of the magnetic particle brake alone is 2.8 and 1.8 Nm for the knee and hip joint. Coupled with the 16:1 transmission, the brake had a holding torque of 44.8 and 28.8 Nm for the knee and hip joint. The weight of these magnetic particle brakes for the knee and hip coupled with a 16:1 transmission is 0.5 and 0.4 kilograms. This is 87:1 and 82:1 Nm of holding torque per kilogram for the case of the magnetic particle brake coupled with a transmission for the knee and hip joint.

The commercial wrap spring brake had a holding torque of 56.5 Nm with a weight of 3.2 kilograms producing 18:1 Nm of holding torque per kilogram. The weight of the commercial wrap spring brake is high in the application where four wrap spring brakes are needed for the system as a whole. A custom designed wrap spring brake is a much more viable option in terms of the weight requirement as it optimizes the weight while maintaining an adequate holding torque. The custom wrap spring brake that was designed for the knee and hip joint had a holding torque value of 33 and 36 Nm while weighing 0.25 kilograms each. This equates to 133:1 and 145:1 Nm of holding torque per kilogram for the case of the custom designed wrap spring brake at the knee and hip joint.

Table 4.1. Holding torque per weight for the brakes. The ratchet has the highest torque to weight ratio, by a substantial amount.

Brake	Holding Torque per Weight (Nm/kg)
WSB Commercial	18:1
WSB Custom (Hip)	145:1
WSB Custom (Knee)	133:1
MPB Commercial	7:1
MPB w/Transmission (Hip)	82:1
MPB w/Transmission (Knee)	87:1
Ratchet	3434:1

The commercial wrap spring brake has a higher holding torque per kilogram of weight compared to the commercial magnetic particle brake by a factor of 2.5 (Table 4.1). The wrap spring brake provides a higher holding torque value per unit of weight. The magnetic particle brakes coupled with transmissions provide a higher holding torque per kilogram of weight compared to the commercial magnetic particle brake by a factor of 12. The custom wrap spring brakes also provide a higher holding torque per kilogram of weight compared to the commercial wrap spring brake by a factor of 8.

The holding torque versus weight for the commercially available magnetic particle brakes from one vendor showed that the holding torque increases with the weight of the brake. The magnetic particle brake's peak torque per weight is 3.8 Nm per kilogram as taken from a trendline fit to data (Figure 3.2). The holding torque versus weight for the commercially available wrap spring brakes from one vendor also showed that the holding torque generally increases with the weight of the brake. The wrap spring brake's peak torque per weight is 44 Nm per kilogram as taken from a trendline fit to data (Figure 3.3).

The holding torque versus weight for a direct drive magnetic particle brake and magnetic particle brakes coupled with various transmission ratios and pitches to satisfy a holding torque requirement of 50 Nm was analyzed. A direct drive magnetic particle brake that has a holding torque of at least 50 Nm was analyzed for reference and to further show that a commercial magnetic particle brake alone would not be feasible for this particular application of a lower limb wearable robotic system due to its high weight. The weight of the commercial magnetic particle brake itself at 14 kilograms makes this option completely impractical for this application.

A smaller magnetic particle brake with a lower holding torque needed to be coupled with a 30:1 transmission to produce a 50 Nm holding torque. A 24 pitch and 18 pitch transmission was analyzed and the higher 24 pitch 30:1 transmission was shown to be less weight than that of the 18 pitch 30:1 transmission. This was also the case for a larger magnetic particle brake with a higher holding torque that needed to be coupled to a 13:1 transmission to produce a 50 Nm holding torque. The magnetic particle brakes coupled with the 18 pitch transmissions weighed more than that of the magnetic particle brakes coupled with the 24 pitch transmissions by a factor of two. These results showed that magnetic particle brakes coupled with a transmission consisting of gears with a higher pitch were more weight efficient compared to being coupled with a transmission consisting of gears with a lower pitch. These results also showed that a magnetic particle brake that required being coupled with a lower gear transmission ratio, 13:1 in this case, produced a higher holding torque to weight compared to that of a magnetic particle brake that required being coupled with a higher gear transmission ratio, 30:1 in this case.

4.3 Power Required to Hold Brake in Locked State

The magnetic particle brake is the only brake that requires power to hold the brake in a locked state out of the three types of brakes that were analyzed. The power required was found to increase as the holding torque increased. The magnetic particle brake's peak power per holding torque is 0.2 Watts per Nm as taken from a linear fit to data shown in Figure 3.5. The commercial magnetic particle brake that was analyzed showed that it required 0.4 Watts per Nm .

For the design of a lower limb wearable robotic system, untethered power is a crucial component and thus, batteries are looked to provide the necessary power required to hold the joint brake and specifically the magnetic particle brakes in their locked state. A lithium-ion battery is a type of rechargeable battery that has the greatest electrochemical potential and provides the largest energy density. Lithium is also the lightest of all metals making this type of battery the most attractive option for this application.

Since battery power is the amount of electrical energy stored in the battery, as more power is required that means that a larger power source is also required which adds weight to the overall robotic system. In this particular application, four magnetic particle brakes are required at each joint. For the case of the commercial magnetic particle brake that was analyzed, the four brakes consume 168 W of electrical power. For the case of the magnetic particle brake coupled with the transmission that was analyzed, the four brakes consume 27 W of electrical power. Practical versions of a lower limb wearable robotic system need brakes with sufficiently low power requirements to enable an hour or more of use on a single battery charge without the power source adding too much weight to the system.

To determine a battery for each of the brakes, the battery capacity must first be determined using the load current of the magnetic particle brake in amps and the desired battery life in hours which

in this case was determined to be one hour of quiet standing which means that the four brakes are energized continuously. One hour was selected as the application of lower limb wearable robotic systems is intended for exercise rather than all-day use and one hour falls within a reasonable range for how long the device may be used for exercise by an individual at one time before the device needs to be recharged. If it is later determined that the device must be used for a longer period of time then the calculations (Appendix E) should be updated to reflect that. The calculated battery capacities and required voltages were used to select a battery (Table 4.2).

Table 4.2. Load current, battery life, battery capacity and weight of the commercial lithium-ion batteries that were selected for analysis

Brake	Load Current (A)	Voltage (V)	Battery Life (Hours)	Battery Capacity (Ah)	Battery Weight (g)
MPB Commercial	2.0	21	1	2.0	351
MPB w/Transmission (Hip)	0.35	10	1	0.35	180
MPB w/Transmission (Knee)	0.35	28	1	0.35	648

A single battery can power all four brakes within the system. For the case of the magnetic particle brake without a transmission, the weight from the battery would be 351 grams. For the case of the magnetic particle brakes coupled with the transmission at the hip and knee, the total weight of the batteries would be 180 and 648 grams. Given that the most previous iteration of the FES-ESO had a design requirement that the weight of the system must be under 10 kilograms, the weight contribution from the batteries themselves are reasonable.

While minimizing weight is an important objective for this application, desirable dimensions and volume of the battery that provided sufficient battery capacity for the analyzed magnetic particle brakes is also important. The dimensions of the AOBEN (Part No. AB7309-C) battery selected for the case of the commercial magnetic particle brake is 12.8 x 8.4 x 8.0 cm producing a volume of 860 centimeters cubed. The dimensions of the AUTEC Power Systems (Part No. APS 28-LIR18650-2.3Ah) battery selected for the case of the magnetic particle brake coupled with a transmission at the hip are a18.4 mm diameter with a 64 mm length producing a volume of 17 centimeters cubed. The dimensions of the EMBRACE SUN (Part No, B09SZ5RZD2) battery selected for the case of the magnetic particle brake coupled with a transmission at the knee is 13.2 x 8.4 x 6.2 cm producing a volume of 687 centimeters cubed.

The volume of the battery selected for the case of the magnetic particle brake coupled with a transmission at the hip is 50 times smaller than the battery selected for the case of the commercial magnetic particle brake alone and 40 times smaller than the battery selected for the case of the magnetic particle brake coupled with a transmission at the knee. This further shows the advantage in weight and volume in using a transmission system coupled to a magnetic particle brake rather than a magnetic particle brake alone to satisfy the torque requirement in the application of a lower limb wearable robotic system.

4.4 Case Study: FES-ESO

Results from this study were applied to the current FES-ESO that was described in Section 1.2 with the objective of selecting the best locking joint. Characteristics that differentiate each of the three brakes were considered in addition to the metrics considered in Sections 4.1, 4.2, and 4.3, as well as the volume, shape, and weight for each brake, and user safety.

The way that the brake fails is an important factor to consider for user safety and when determining how big of a factor of safety to include. Magnetic particle brakes, wrap spring brakes, and ratchet brakes are passive devices with no possibility of human injury resulting from unstable behavior and are therefore well suited for uses involving human interaction. An advantage of wrap springs and ratchets over magnetic particle brakes is that the unpowered position locks the joint which will prevent the collapse of the user if power failure of the device occurs. When torque is exceeded in the case of the magnetic particle brake, the brake will slip without jerking. The magnetic particle brake is not in a locked state when no power is applied which can lead to a catastrophic failure in the case of a power failure. For a ratchet, when no power is applied it is also in the locked state. Therefore, while all three of these devices are passive contributing to user safety, only the wrap spring brake and ratchet brake are in the locked position with no power preventing a catastrophic failure while the magnetic particle brake is not.

The weight of the ratchet can be minimized by only using the internal components of the ratchet with custom housing. Another advantage of this beyond weight is that the shape of the brake and joint can be tailored to provide a user-friendly fit to help improve user experience. A wrap spring brake can be custom designed and manufactured to optimize the weight of the brake. An optimized wrap spring is one of minimum volume and thus weight meaning the least axial width and least radius. A magnetic particle brake is much more intensive to manufacture due to the complexity of the mechanism itself. However, weight can be optimized by customizing the gears used within the transmission selected to be coupled with the magnetic particle brake. The gears used in the transmission only actuate through specified angles so all other gear teeth will never mesh. Therefore, these parts of the gear can be removed while still allowing material for mounting on the shaft. Additional weight can also be removed by drilling holes in the remaining part of the gear as long as enough material is left for the needed part strength.

The overall shape of the brake is important to consider. The weight and volume optimized custom wrap spring brake used in a previous FES-ESE iteration resulted in a two inch or five cm decrease in the outward projection of the brace on the sides compared to the magnetic particle brake used in a previous CBO iteration (Figure 4.1).

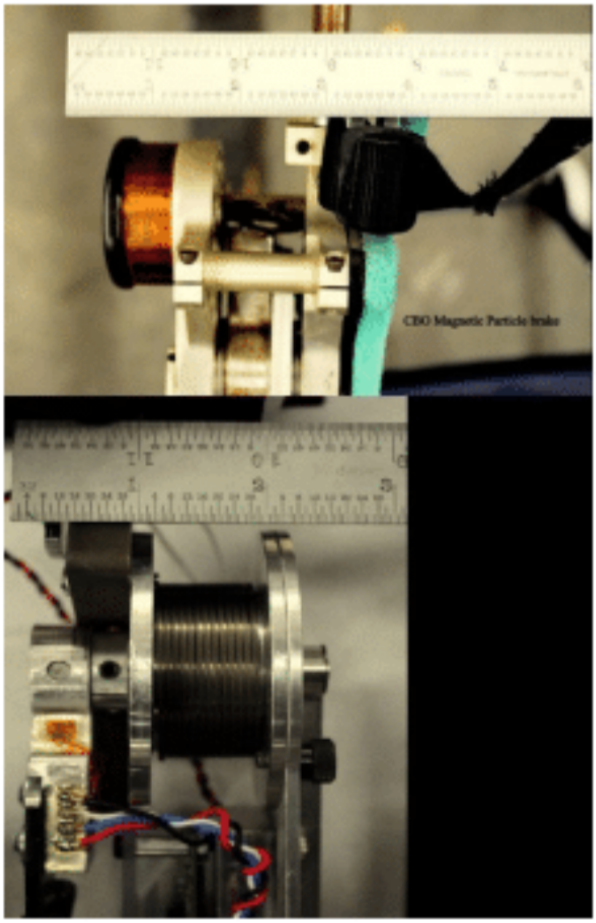

Figure 4.1. A visual comparison of the outward projection between the magnetic particle brakes used in the CBO [40] (top image) and the wrap spring brakes used in the FES-ESE [44] (bottom image).

Brake Recommendation for FES-ESO

While the wrap spring is light, strong, and requires zero power, it does not work with this application due to the slip and subsequent sag that occurs before the brake completely locks. To accomplish a gait cycle it is not necessary to accurately achieve prescribed angles, but sagging occurred while standing which put the user in a crouched posture that was unacceptable. Ensuring that there is sufficient toe clearance during the swing phase is also a major challenge due to the sagging.

While the ratchet can be easily weight and volume optimized through customization of the housing and provides high holding torque, the three degrees swing arc leads to backlash and sagging, the switching time between states is slow, and the loud, audible noise while ratcheting and lack of smooth engagement as the ratchet is ratcheting is unacceptable for the user experience in this application.

Therefore, given the analysis conducted the magnetic particle brake was determined to be the best locking joint for the FES-ESO system out of the three brake types analyzed. The primary differentiating advantages for using the magnetic particle brakes are the relatively high holding torque to weight ratios when coupled with a transmission and the shape and weight of the gears can be reduced due to only needing limited ranges of motion for this application. The magnetic particle brake does this while providing smooth and quiet engagement which is optimal for the user's experience.

While a power source is needed in the case of the magnetic particle brake, it is possible and recommended to explore a magnetic particle brake with a transmission coupled with a releasable lock in order to turn off the magnetic particle brake when the user is in the quiet standing position and use the lock. This would decrease the need for a power to lock the brake in its holding state and therefore decrease the size needed of the power source which in turn decreases the overall weight of the power source and system.

To further optimize the weight of the system, it is possible to use different magnetic particle brakes for the hip and knee joints respectively based on the holding torque required at each joint. In the torque analysis conducted above, it was found that the hip joint was subject to a much lower holding torque compared to the knee torque. A magnetic particle brake with a lower holding torque requirement and therefore a lower weight could then be used in the case of the hip joints compared to the brake that would be required at the knee joint.

Chapter 5. Conclusions

In the analysis of a magnetic particle brake, wrap spring brake, and ratchet brake, the torque requirement was found to be greater in the knee joint compared to the hip joint. The torque requirement was also at a maximum in the working phases or single support phase of gait compared to the torque requirement in the case of quiet standing. It was also found that the holding torque increases with the weight of the brake. The ratchet brake had the highest holding torque in Nm to weight in kilograms with the custom wrap spring brakes, commercial wrap spring brakes, magnetic particle brakes with transmission. then the commercial magnetic particle brake following. The power required to hold a magnetic particle brake in its locked state was found to increase as the holding torque increased. Based on these conclusions and the analysis

conducted above, the magnetic particle brake was determined to be the best locking joint for the FES-ESO system out of the three brake types analyzed. Before implementing into the system, the use of a releasable lock to turn off the magnetic particle brake when the user is in the quiet standing phase in order to minimize the size of the power source that is required.

References

[1] C. H. Ho, R. J. Triolo, A. L. Elias, K. L. Kilgore, A. F. DiMarco, K. Bogie, A. H. Vette, M. L. Audu, R. Kobetic, S. R. Chang, K. M. Chan, S. Dukelow, D. J. Bourbeau, S. W. Brose, K. J. Gustafson, Z. H. Kiss, and V. K. Mushahwar, “Functional electrical stimulation and spinal cord injury,” *Phys Med Rehabil Clin N Am*, vol. 25, no. 3, pp. 631–654, 2014.

[2] A. J. del Ama, J. C. Moreno, Á. Gil-Agudo, and J. L. Pons, “Hybrid fes-robot cooperative control of ambulatory gait rehabilitation exoskeleton for spinal cord injured users,” *Biosystems & Biorobotics*, pp. 155–159, 2013.

[3] E. Brown, Y. F. Ullah, K. Gustafson, and W. Durfee, “Preliminary design of muscle-powered exoskeleton for users with Spinal Cord Injury,” *2022 Design of Medical Devices Conference*, 2022.

[4] “Spinal Cord Injury (SCI) 2016 facts and figures at a glance,” *The Journal of Spinal Cord Medicine*, vol. 39, no. 4, pp. 493–494, 2016.

[5] E. A. Kruger, M. Pires, Y. Ngann, M. Sterling, and S. Rubayi, “Comprehensive management of pressure ulcers in spinal cord injury: Current concepts and future trends,” *The Journal of Spinal Cord Medicine*, vol. 36, no. 6, pp. 572–585, 2013.

[6] Nene, A. V., and Patrick, J. H., "Energy cost of paraplegic locomotion with the ORLAU ParaWalker," *Paraplegia*, 27(1), pp. 5-18, 1989.

[7] Summers, B. N., McClelland, M. R., and el Masri, W. S., "A clinical review of the adult hip guidance orthosis (Para Walker) in traumatic paraplegics," *Paraplegia*, 26(1), pp. 19-26, 1988.

[8] Filho, R. M. C., Tamburus, W. M., and Carvalho, J., "Case report: Para Walker ambulation for adult tetraplegic patients: Two case reports," *Prosthetics and Orthotics International*, 25(1), pp. 71-74, 2001.

[9] Lyles, M., and Munday, J., "Report on the evaluation of the Vannini-Rizzoli Stabilizing Limb Orthosis," *J Rehabil Res Dev*, 29(2), pp. 77-104, 1992.

[10] A. A. Rasmussen, K. M. Smith, and D. L. Damiano, “Biomechanical evaluation of the combination of bilateral stance-control knee-ankle-foot orthoses and a reciprocating gait orthosis in an adult with a spinal cord injury,” *JPO Journal of Prosthetics and Orthotics*, vol. 19, no. 2, pp. 42–47, 2007.

[11] J. W. Barnes, D. K. Sager, and A. C. Higgins, “Case Study: The Use of Bail Lock Knee Joints in the Rehabilitation of the High Level Spinal Cord Injured Below-Knee Amputee ,” *Orthotics and Prosthetics*, vol. 40, no. 4, 1987.

[12] C. A. Yee, "Hip Actuation Designs to Support the Back while Stooping and Walking." Order No. 10188365, University of California, Berkeley, Ann Arbor, 2016.

[13] S. E. Irby, K. R. Kaufman, R. W. Wirta, and D. H. Sutherland, “Optimization and application of a wrap-spring clutch to a dynamic knee-ankle-foot orthosis,” *IEEE Transactions on Rehabilitation Engineering*, vol. 7, no. 2, pp. 130–134, 1999.

[14] G. Chen, C. K. Chan, Z. Guo, and H. Yu, “A review of lower extremity assistive robotic exoskeletons in rehabilitation therapy,” Crit Rev Biomed Eng, vol. 41, no. 4-5, pp. 343–363, 2013.
[15] M. Talaty, A. Esquenazi, and J. E. Briceno, “Differentiating ability in users of the rewalk powered exoskeleton: An analysis of walking kinematics,” *2013 IEEE 13th International Conference on Rehabilitation Robotics (ICORR)*, 2013.
[16] D. Duddy, R. Doherty, J. Connolly, J. Loughrey, J. Condell, D. Hassan, and M. Faulkner, “The cardiorespiratory demands of treadmill walking with and without the use of Ekso GT™ within able-bodied participants: A feasibility study,” *International Journal of Environmental Research and Public Health*, vol. 19, no. 10, p. 6176, 2022.
[17] K. J. Nolan, K. K. Karunakaran, P. Roberts, C. Tefertiller, A. M. Walter, J. Zhang, D. Leslie, A. Jayaraman, and G. E. Francisco, “Utilization of robotic exoskeleton for Overground walking in acute and chronic stroke,” *Frontiers in Neurorobotics*, vol. 15, 2021.
[18] L. Miller, A. Zimmermann, and W. Herbert, “Clinical effectiveness and safety of powered exoskeleton-assisted walking in patients with spinal cord injury: Systematic review with Meta-analysis,” *Medical Devices: Evidence and Research*, p. 455, 2016.
[19] D. R. Louie, J. J. Eng, and T. Lam, “Gait speed using powered robotic exoskeletons after Spinal Cord Injury: A systematic review and Correlational Study,” *Journal of NeuroEngineering and Rehabilitation*, vol. 12, no. 1, 2015.
[20] A. R. Kralj and T. Bajd, “Functional electrical stimulation: Standing and walking after Spinal Cord Injury,” 1989.
[21] “Parastep I™ system,” Parastep I™ System | Sigmedics Inc. [Online]. Available: https://www.sigmedics.com/parastep-i-system. [Accessed: 10-Nov-2022].
[22] T. D. Lavis and L. Codamon, “Lower limb orthoses for persons with Spinal Cord Injury,” *Atlas of Orthoses and Assistive Devices*, 2019.
[23] A. Kralj et al. Gait restoration in paraplegic patients: A feasibility demonstration using multichannel surface electrodes. *Journal of Rehabilitation Research and Development*, 20(1):3-20, 1983.
[24] A. Kralj and T. Bajd. FES:standing and walking after Spinal Cord Injury. *CRC Press*, 1989.
[25] Kralj, A., Bajd, T., and Turk, R., " Electrical stimulation providing functional use of paraplegic patient muscles," *Med. Prog.Technol*., 7, pp. 3-9, 1980.
[26] Bajd, T., Kralj, A., Turk, R., Benko, H., and Sega, J, "The use of a fourchannel electrical stimulator as an ambulatory aid for paraplegic patients," *Phys Ther*, 63(7), pp. 1116-1120, 1983.
[27] Kobetic, R., and Marsolais, E. B., "Synthesis of paraplegic gait with multichannel functional neuromuscular stimulation," *Rehabilitation Engineering, IEEE Transactions* on, 2(2), pp. 66-79, 1994.
[28] Goldfarb, M., "A Controlled-Brake Orthosis for FES-Aided Gait," Ph.D., *Massachusetts Institute of Technology*, 1993.

[29] Popovic, D., Tomovic, R., and Schwirtlich, L., "Hybrid assistive system-the motor neuroprosthesis," *Biomedical Engineering*, *IEEE Transactions* on, 36(7), pp. 729-737, 1989.

[30] Andrews, B. J., "A modular hybrid fes orthosis for paraplegics," *Proc. Engineering In Medicine And Biology*, pp. 2256-2257.

[31] Andrews, B. J., and Kirkwood, C. A., "Control of hybrid FES orthoses," pp.1473 - 1474, 1989.

[32] Gharooni, S., Heller, B., and Tokhi, M. O., "A new hybrid spring brake orthosis for controlling hip and knee flexion in the swing phase," *IEEE Trans Neural Syst Rehabil Eng*, 9(1), pp. 106-107, 2001.

[33] Kagaya, H., Shimada, Y., Sato, K., Sato, M., Iizuka, K., and Obinata, G., "An electrical knee lock system for functional electrical stimulation," *Archives of Physical Medicine and Rehabilitation,* 77(9), pp. 870-873, 1996.

[34] Marsolais, E. B., Kobetic, R., Polando, G., Ferguson, K., Tashman, S., Gaudio, R., Nandurkar, S., and Lehneis, H. R., "The Case Western Reserve University hybrid gait orthosis," *J Spinal Cord Med*, 23(2), pp. 100-108, 2000.

[35] To, C. S., Kirsch, R. F., Kobetic, R., and Triolo, R. J., "The feasibility of a functional neuromuscular stimulation powered mechanical gait orthosis with coordinated joint locking," *Conf Proc IEEE Eng Med Biol Soc*, 6, pp. 4041-4044, 2004.

[36] To, C. S., Kirsch, R. F., Kobetic, R., and Triolo, R. J., "Simulation of a functional neuromuscular stimulation powered mechanical gait orthosis with coordinated joint locking," *IEEE Trans Neural Syst Rehabil Eng*, 13(2), pp. 227-235, 2005.

[37] To, C. S., Kobetic, R., Schnellenberger, J. R., Audu, M. L., and Triolo, R. J., "Design of a Variable Constraint Hip Mechanism for a Hybrid Neuroprosthesis to Restore Gait After Spinal Cord Injury," *IEEE/ASME Transactions on Mechatronics*, 13(2), pp. 197-205, 2008.

[38] Kobetic, R., To, C. S., Schnellenberger, J. R., Audu, M. L., Bulea, T. C., Gaudio, R., Pinault, G., Tashman, S., and Triolo, R. J., "Development of hybrid orthosis for standing, walking, and stair climbing after spinal cord injury," *J Rehabil Res Dev*, 46(3), pp. 447-462, 2009.

[39] Farris, R. J., Quintero, H. A., Withrow, T. J., and Goldfarb, M., "Design of a joint-coupled orthosis for FES-aided gait," *2009 IEEE International Conference on Rehabilitation Robotics*, pp. 246-252, 2009.

[40] M. Goldfarb and W. K. Durfee, “Design of a controlled-brake orthosis for fes-aided gait,” *IEEE Transactions on Rehabilitation Engineering*, vol. 4, no. 1, pp. 13–24, 1996.

[41] W. K. Durfee and A. Rivard, “Design and simulation of a pneumatic, stored-energy, hybrid orthosis for gait restoration,” *J Biomech Eng*, vol. 127, no. 6, pp. 1014–1019, 2005.

[42] A. Kangude, B. Burgstahler, J. Kakastys, and W. Durfee, “Single channel hybrid FES gait system using an energy storing orthosis: preliminary design,” *Conf Proc IEEE Eng Med Biol Soc*, vol. 2009, pp. 6798–6801, 2009.

[43] A. Kangude, B. Burgstahler, and W. Durfee, “Engineering evaluation of the energy-storing orthosis FES gait system,” *Conf Proc IEEE Eng Med Biol Soc*, vol. 2010, pp. 5927–5930, 2010.
[44] K. Boughner, “Design of an energy storing orthosis for providing gait to people with spinal
cord injury,” Master’s thesis, University of Minnesota, 2014.
[45] R. Borgeson, E. Dozier, T. Borowicz, A. Caceres, and S. Thole, “Energy storing orthosis design,” University of Minnesota, Capstone Design Report, 2015.
[46] A. Campos, “Design of an elastic storing orthosis,” University of Minnesota, Technical Report, 2016.
[47] S. E. Irby, K. R. Kaufman, R. W. Wirta, and D. H. Sutherland, “Optimization and application of a wrap-spring clutch to a dynamic knee-ankle-foot orthosis,” *IEEE Transactions on Rehabilitation Engineering*, vol. 7, no. 2, pp. 130–134, 1999.
[48] Sepac, “Customizing a wrap spring clutch or brake to your medical application,” SEPAC, Inc, 22-Aug-2022. [Online].
[49] C. F. Wiebusch, “The Spring Clutch,” *Journal of Applied Mechanics*, vol. 6, no. 3, 1939.
[50] “How magnetic particle brakes work > placid industries,” Placid Industries, 21-Dec-2020. [Online].
[51] “Tension Control Systems for Light, Medium, and Heavy-Duty Tensioning,” Tension Control Systems for Light, Medium, and Heavy-Duty Tensioning - WARNER ELECTRIC - PDF Catalogs | Technical Documentation | Brochure, Mar-2021. [Online]. Available: https://pdf.directindustry.com/pdf/warner-electric/tension-control-systems-light-medium-heavy-duty-tensioning/4820-818813.html. [Accessed: 04-Jan-2023].
[52] B. Becker, “Selecting the Right Tensioning System for the Application,” PFF - Paper, Film & Foil Converter, 01-May-2020. [Online]. Available: https://www.pffc-online.com/magazine/298-paper-selecting-right-tensioning. [Accessed: 10-Nov-2022].
[53] V. V. Katti, "Design of a Muscle-Powered Walking Exoskeleton for People with Spinal Cord Injury." Order No. 10846254, University of Minnesota, United States -- Minnesota, 2018.
[54] Socket Wrenches, Handles, and Attachments B107.110 - 2019. *ASME*, 2020.
[55] Winter, D. A., 2009, Biomechanics and Motor Control of Human Movement, Wiley, Hoboken, N.J.

Appendices

A. Failure Torque Calculations

a. Free Body Diagram Analysis

The failure torque values were calculated for an individual of weight 111.58 kilograms and height of 1.88 meters using Winter's anthropometric regression models [55]. The general free body diagram showing all terms drawn and defined (Figure A.1).

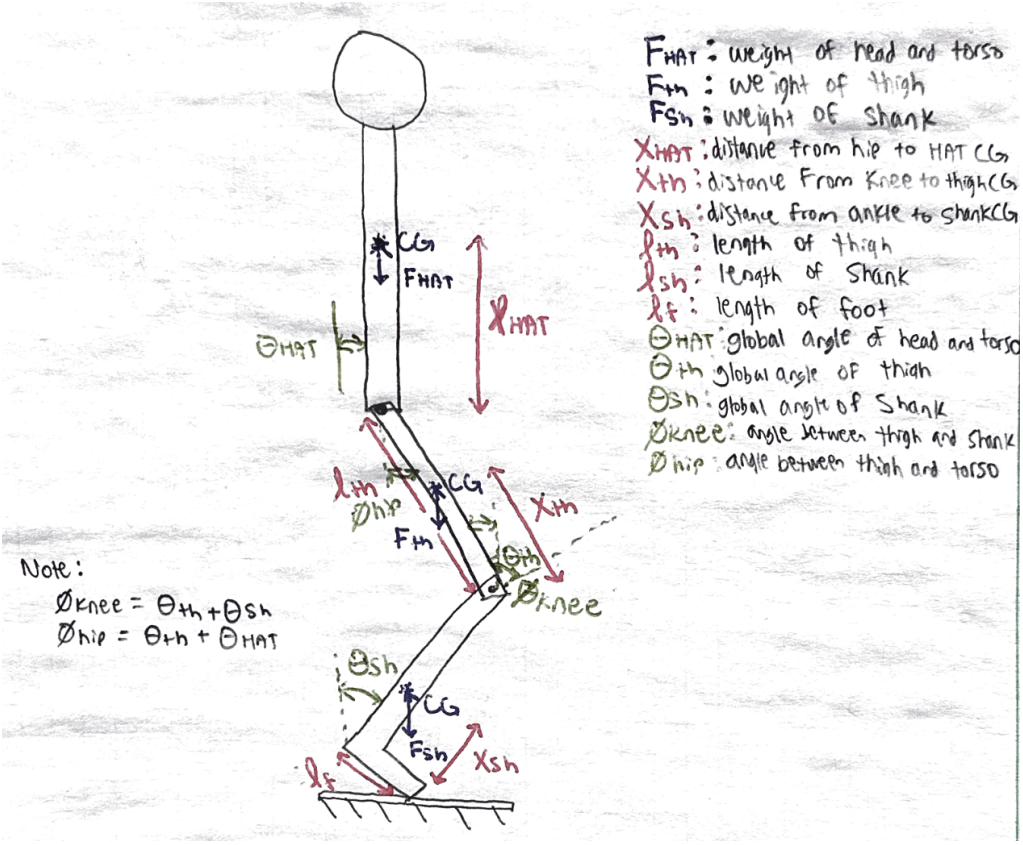

Figure A.1. General free body diagram illustrating the relevant lengths, distances, forces, and angles and describing what they mean.

Quiet Standing

For summing torques about the knee, the shank is held fixed.

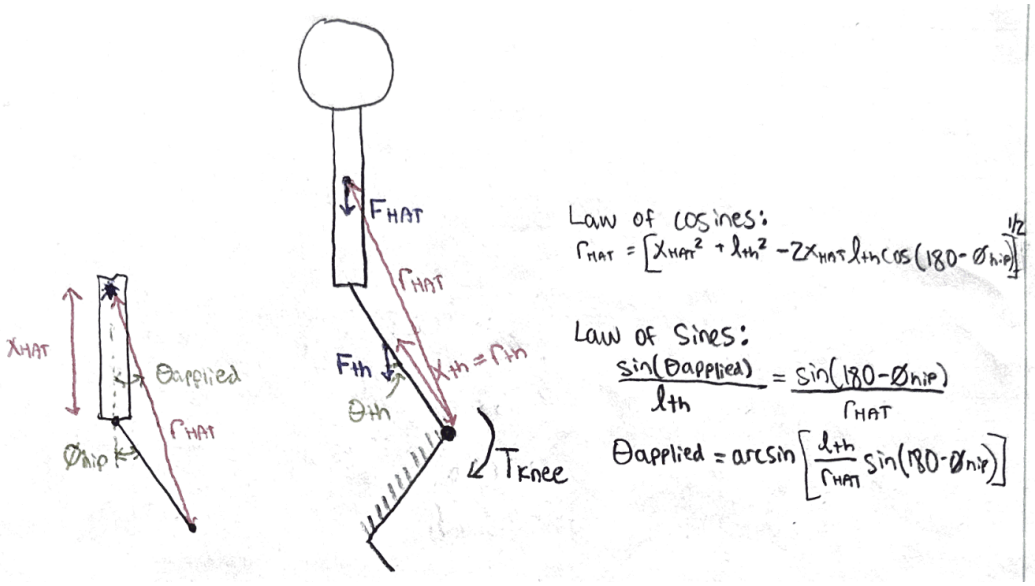

Figure A.2. Free body diagram used for calculating the knee torque in quiet standing and relevant definitions of terms.

The Law of Cosines is used to define r_{HAT} as:

$$r_{HAT} = [x_{HAT}^2 + l_{th}^2 - 2x_{HAT}l_{th}cos(180 - \phi_{Hip})]^{1/2}$$

The Law of Sines is used to define $\theta_{applied}$ as:

$$\frac{sin(\theta_{applied})}{l_{th}} = \frac{sin(180-\phi_{Hip})}{r_{HAT}}$$

$$\theta_{applied} = arcsin[\frac{l_{th}}{r_{HAT}} sin(180 - \phi_{Hip})]$$

By summing the torques about the knee, the following equation for the torque at the knee joint in quiet standing is produced:

$$T_{KNEE} = x_{th}F_{th}sin(\phi_{Hip}) + r_{HAT}\left(\frac{F_{HAT}}{2}\right)sin(\theta_{applied})$$

For summing torques about the hip, the thigh is held fixed. Note that r_{HAT} is defined differently than in the case of knee torque analysis since it is now defined as the distance from the HAT center of mass to the hip joint rather than the knee joint otherwise known as x_{HAT}

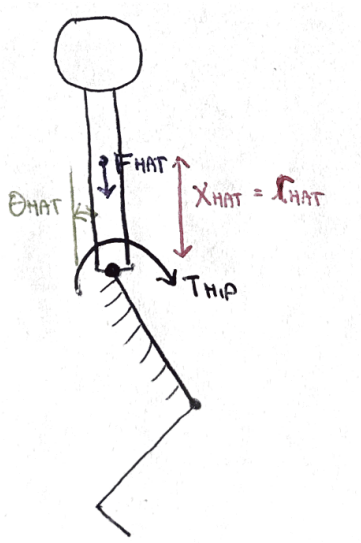

Figure A.3. Free body diagram used for calculating the hip torque in quiet standing.

By summing the torques about the hip, the following equation for the torque at the hip joint in quiet standing is produced:

$$T_{HIP} = r_{HAT}\left(\frac{F_{HAT}}{2}\right)sin\theta_{HAT}$$

Note that these equations produce the total torque acting about a single hip and knee joint respectively as an assumption is made that the weight is being equally distributed between the two legs.

Working Phases

For summing torques about the knee, the shank is held fixed. In this case, an additional force is acting on the hip joint from the weight of the leg that is off the ground.

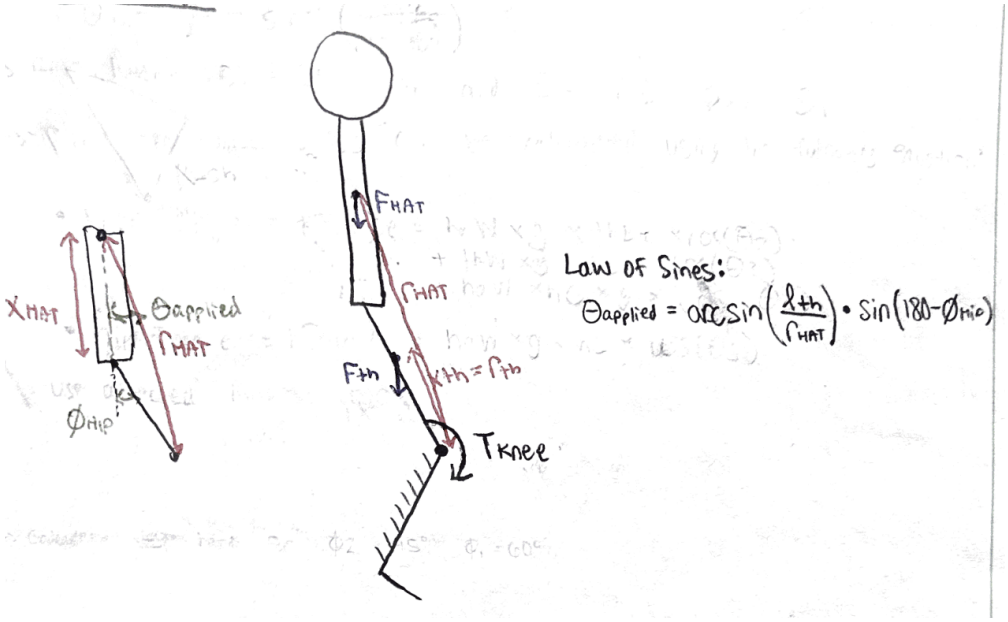

Figure A.4. Free body diagram used for calculating the knee torque in working phases and relevant definitions of terms.

The applied angle in this case is found in the same manner as in the case of quiet standing through the Law of Sines.

$$\theta_{applied} = arcsin[\frac{l_{th}}{r_{HAT}} sin(180 - \phi_{Hip})]$$

To account for the force of the leg that is off the ground, the thigh and shank of that leg is added to the force due to the total head and torso since all of that force is acting on the leg that is on the ground. By summing the torques about the knee, the following equation is produced for the torque at the knee joint in the phase(s) of the gait cycle in which one leg is on the ground and one leg is off:

$$T_{KNEE} = x_{th} F_{th} sin(\phi_{Hip}) + r_{HAT}(F_{HAT} + F_{sh} + F_{th}) sin(\theta_{applied})$$

For summing torques about the hip, the thigh is held fixed. In this case, an additional force is acting on the hip joint from the weight of the leg that is off the ground.

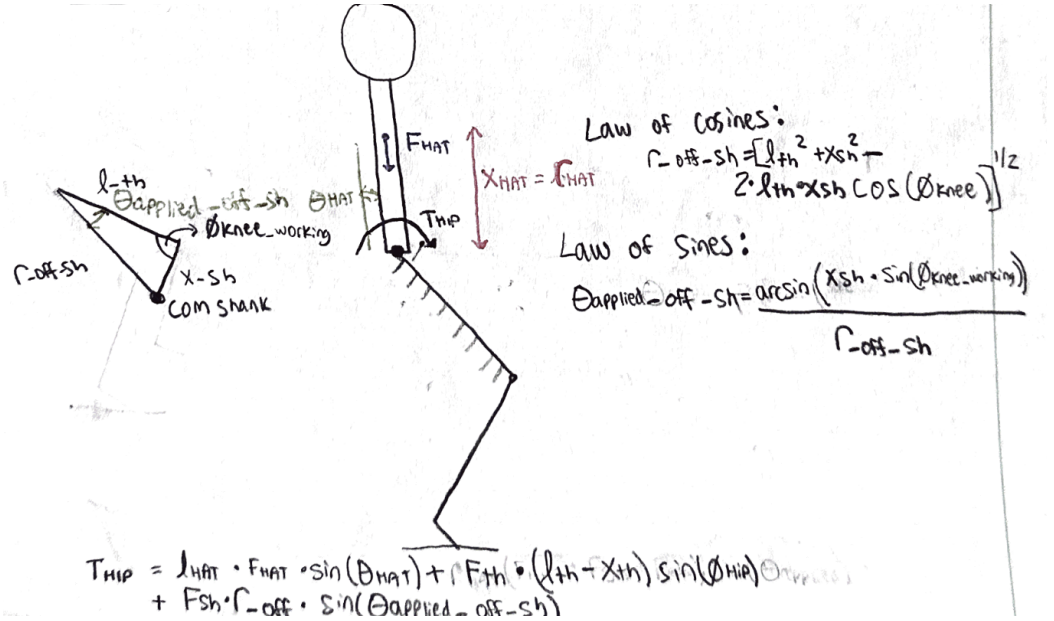

Figure A.5. Free body diagram used for calculating the hip torque in working phases and relevant definitions of terms.

The Law of Cosines is used to define $r_{off_{shank}}$ as:

$$r_{off_{sh}} = [l_{th}^2 + x_{sh}^2 - 2l_{th}x_{sh}cos(\phi_{knee})]^{1/2}$$

The Law of Sines is used to define $\theta_{applied_{offshank}}$ as:

$$\theta_{appled_{offsh}} = \frac{arcsin(x_{sh}sin(\phi_{knee_{working}})}{r_{off_{shank}}}$$

By summing the torques about the hip, the following equation is produced for the torque at the hip joint in the working phases of the gait cycle in which one leg is on the ground and one leg is off:

$$T_{HIP} = r_{HAT}F_{HAT}sin(\theta_{HAT}) + F_{th}(l_{th} - x_{th})sin(\phi_{Hip}) + F_{sh}r_{off_{sh}}sin(\theta_{applied_{offsh}})$$

b. MATLAB Code

```
clc; close; clear;
%Author: Emily Brown
%Date: 12/8/2022

%All data Anthropometric data from Winter's biomechanics book
%Assumptions
%Subject Height - 1.88 m
%Weight - 111.58 kg

theta_HAT = 0;                                                  %Assume HAT always vertical

h = 1.88;                                                       %Total height in m
m = 111.58;                                                     %Total mass in kg
g = 9.81;                                                       %Acceleration due to gravity to convert kg to N (m/s^2 )

%Fraction weights from Winter
f_total_leg = 0.061;
f_thigh = 0.100;
f_HAT = 0.678;

%Weights and forces
W_shank = f_total_leg * m;                                      %Shank weight in kgs (multiply by 0.4536 to convert lb to kg)
W_thigh = f_thigh * m;                                          %Thigh weight
W_HAT = (f_HAT * m);                                            %HAT weight

F_HAT = W_HAT * g;                                              %F = ma
F_thigh = W_thigh * g;                                          %F = ma
F_shank = W_shank * g;

%Fraction heights from Winter
l_shank = (0.285 - 0.039) * h;                                  %Shank length in m (multiply by 0.0254 to convert in to m)
l_thigh = (0.530 - 0.285) * h;                                  %Thigh Length in m
l_HAT = (0.870 - 0.530) * h;                                    %HAT length in m
l_foot = 0.152 * h * 0.0254;                                    %Foot length in sagittal plane

%Distance of COM from joints
x_shank = 0.394 * l_shank;                                      %Distance of COM of shank from malleolus (ankle)
x_thigh = 0.567 * l_thigh;                                      %Distance of COM of thigh from femoral condyles (knee)
x_HAT = 0.626 * l_HAT;                                          %Distance of COM of HAT from greater trochanter (hip)
```

```
%Angle Range of Hip and Knee
hip_min = -21;
hip_max = 21;
hip_quiet_max = 10;
knee_min = 0;
knee_max = 60;
hip_num = 10;                                                   %Number of hip angles evaluated
knee_num = 10;                                                  %Number of knee angles evaluated

%Vector Definitions
Htheta_quiet = linspace(0,hip_quiet_max,hip_num);
Htheta = linspace(0,hip_max,hip_num);
Hphi_quiet = Htheta_quiet+theta_HAT;                            %Assume HAT vertical
Hphi = Htheta+theta_HAT;
% Hphi_quiet = -(Htheta_quiet - theta_HAT);
% Hphi = -(Htheta - theta_HAT);
theta_off_hip = linspace(0,hip_max,hip_num);                    %Global hip angle of leg off ground
theta_off_knee = linspace(0,knee_max,hip_num);                  %Global knee angle of leg off ground

%Vector Initializations
Kphi_quiet = zeros(1,hip_num);                                  %Quiet standing relative knee angle
T_hip_quiet = zeros(1,hip_num);                                 %Quiet standing torque at hip
T_knee_quiet = zeros(1,hip_num);                                %Quiet standing torque at knee
Kphi_working = zeros(1,length(Htheta));                         %Working relative knee angle
T_hip_working = zeros(hip_num,hip_num);                         %Working torque at hip
T_knee_working = zeros(hip_num,hip_num);                        %Working torrque at knee
```

```
%%%%%%%%%%%%%%%%%%%%%%%%%%%%%%%%%%%%%%%%%%%%%%%%%%%%%%%%%%%%%%%%%%%%%%%%%%%
%%%%%%%%%%%%%%%%%%%%%%% QUIET STANDING %%%%%%%%%%%%%%%%%%%%%%%%%%%%%%%%%%%%                             %Index through angles - assume COM falls at center of foot
%%%%%%%%%%%%%%%%%%%%%%%%%%%%%%%%%%%%%%%%%%%%%%%%%%%%%%%%%%%%%%%%%%%%%%%%%%%

for j = 1:length(Hphi_quiet)
    Kphi_quiet(1,j) = 180 - Hphi_quiet(1,j) - asind((l_thigh*sind(Hphi_quiet(1,j)))/l_shank);          %Calculate phi_knee at each hip angle
    r_HAT = sqrt((x_HAT^2)+(l_thigh^2)-(2*x_HAT*l_thigh*cosd(180-Hphi_quiet(1,j))));                    %Law of Cosines for torque lever
    theta_app(1,j) = asind((l_thigh/r_HAT)*sind(180-Hphi_quiet(1,j)));                                  %Law of Sines for applied torque angle
    %Quiet Standing Hip Torque
    T_hip_quiet(1,j) = x_HAT*(F_HAT/2)*sind(theta_HAT);
    %Quiet Standing Knee Torque
    T_knee_quiet(1,j) = x_thigh*F_thigh*sind(Hphi_quiet(1,j))+r_HAT*(F_HAT/2)*sind(theta_app(1,j));
end

scatter(Hphi_quiet,180-Kphi_quiet,[],T_knee_quiet,'filled');
colormap hsv
grid on; hold on;
axis equal
ylim([0 20]); xlim([0 10]); xlabel('Hip Flexion [degrees]'); ylabel('Knee Flexion [degrees]');
colorbar
c = colorbar;
c.Label.String = 'Torque [Newton-meters]';

%%%%%%%%%%%%%%%%%%%%%%%%%%%%%%%%%%%%%%%%%%%%%%%%%%%%%%%%%%%%%%%%%%%%%%%%%%%

%%%%%%%%%%%%%%%%%%%%%%%%%%%%%%%%%%%%%%%%%%%%%%%%%%%%%%%%%%%%%%%%%%%%%%%%%%%
%%%%%%%%%%%%%%%%%%%%%%%%%% WORKING PHASES %%%%%%%%%%%%%%%%%%%%%%%%%%%%%%%%%                             %Index through angles - assume COM falls at center of foot
%%%%%%%%%%%%%%%%%%%%%%%%%%%%%%%%%%%%%%%%%%%%%%%%%%%%%%%%%%%%%%%%%%%%%%%%%%%

for j = 1:length(Hphi_quiet)
    Kphi_quiet(1,j) = 180 - Hphi_quiet(1,j) - asind((l_thigh*sind(Hphi_quiet(1,j)))/l_shank);          %Calculate phi_knee at each hip angle
    r_HAT = sqrt((x_HAT^2)+(l_thigh^2)-(2*x_HAT*l_thigh*cosd(180-Hphi_quiet(1,j)-theta_HAT)));          %Law of Cosines for torque lever
    theta_app(1,j) = asind((l_thigh/r_HAT)*sind(180-Hphi_quiet(1,j)-theta_HAT));                        %Law of Sines for applied torque angle
    for k = 1:hip_num
        r_off_shank = sqrt(l_thigh^2+x_shank^2-(2*l_thigh*x_shank*cosd(Kphi_working(1,k))));
        theta_app_off_shank = (asind(x_shank*sin(Kphi_working(1,k))))/r_off_shank;
        %WORKING PHASES Hip Torque
        T_hip_working(j,k) = x_HAT*F_HAT*sind(theta_HAT)+(F_thigh*(l_thigh-x_thigh)*sind(Hphi(1,k)))+(F_shank*r_off_shank*sind(theta_app_off_shank));
        %WORKING PHASES Knee Torque - note does not change with angle of leg off ground
        T_knee_working(j,k) = x_thigh*F_thigh*sind(Hphi_quiet(1,j))+r_HAT*(F_HAT+F_shank+F_thigh)*sind(theta_app(1,j));
    end
end

%%%%%%%%%%%%%%%%%%%%%%%%%%%%%%%%%%%%%%%%%%%%%%%%%%%%%%%%%%%%%%%%%%%%%%%%%%%
```

```
%Truncate data for quiet standing and working angles
T_knee = [transpose(T_knee_quiet) T_knee_working]
T_hip = [transpose(T_hip_quiet) T_hip_working]

%%%%%%%%%%%%%%%%%%%%%%%%%%%%%%%%%%%%%%%%%%%%%%%%%%%%%%%%%%%%%%%%%%%%%%%%%%%
%%%%%%%%%%%%%%%%%%%%%%%%%%% A-FRAME PHASE %%%%%%%%%%%%%%%%%%%%%%%%%%%%%%%%%
%%%%%%%%%%%%%%%%%%%%%%%%%%%%%%%%%%%%%%%%%%%%%%%%%%%%%%%%%%%%%%%%%%%%%%%%%%%

% %A-FRAME PHASE Hip Torque
% T_hip_A = (((F_HAT/2)+F_shank+F_thigh)*sind(hip_max)*(l_thigh+l_shank)) - (F_thigh*(l_thigh-x_thigh)*sind(hip_max)) - (F_shank*(l_thigh+x_shank)*sind(hip_max))
% %A-FRAME PHASE Knee Torque
% T_knee_A = (((F_HAT/2)+F_shank+F_thigh)*sind(hip_max)*(l_shank)) - (F_shank*(x_shank)*sind(hip_max))
```

B. Data Sheets of Selected Brakes

a. WSB Commercial

Link to Data Sheet - page 18

CB-6 Clutch / Brake

Dimensions in. (mm)

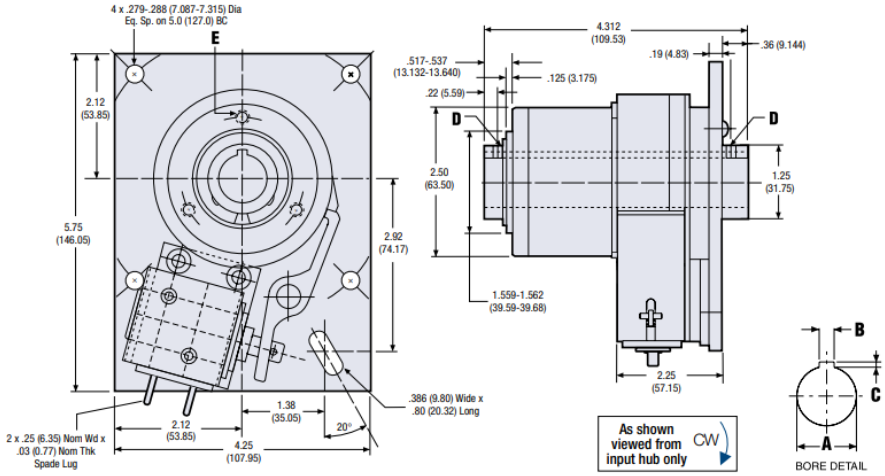

Bore & Keyway Sizes

	Bore A	Keyway Width B	Keyway Depth C	Set Screws/Pin Hole D	Mtg. Holes E
English in.	.7505-.7525	.1875	.09375	2x #10-32 UNF-2B	3x #1/4-20 UNC-2B
(mm)	(19.062-19.114)	(4.7625)	(2.381)		Eq. Sp. on 2.062 BC
	1.0005-1.0025	—	—	2x .187 Hole	3x #1/4-20 UNC-2B
	(25.412-25.464)			(4.7498)	Eq. Sp. on 2.062 BC
Metric mm	20.0 H9	6.0	2.8	2x M5 x 0.8 x 5.0	3x M6 x 1.0 on
(in.)	(.7874-.7894)	(.2362)	(.1102)	Lg. Hex Soc. Set Screw	52.38 BC
	25.0 H9	—	—	2x 5.0 Hole	3x M6 x 1.0 on
	(.9842-.9862)			(.191-.203)	52.38 BC

All dimensions are nominal unless otherwise noted.

CB-6 Part Numbers

Bore Size	Voltage	Rotation	Stops 1	Stops 2	Stops 4
0.75"	24 VDC	CW	306-17-051	306-17-074	306-17-162
		CCW	306-27-029	306-27-046	306-27-134
0.75"	115 VAC	CW	306-17-053	306-17-060	306-17-073
		CCW	306-27-031	306-27-039	306-27-045
1.0"	24 VDC	CW	306-17-057	306-17-061	306-17-031
		CCW	306-27-032	306-27-147	306-27-150
1.0"	115 VAC	CW	306-17-059	306-17-062	306-17-075
		CCW	306-27-034	306-27-044	306-27-037

These are the most commonly requested parts – other voltages (such as 12VDC and 90VDC), bores and stop collars are available.
See page 40 for metric part numbers.

Electrical Data (±10%)

Voltage	Current (amps)	Resistance (ohms)	Status
115 AC 60 Hz	.33*	53.5	Standard
24 DC	.60	39.9	Standard
12 DC	1.15	10.4	Option
90 DC	.15	598	Option

(Coils are rated for continuous duty)
*115 AC-In rush current .62 amps, Holding current .31 amps

Specifications

Static Torque	500 lb.in.
Maximum anti-overrun holding capability	300 lb.in.
Maximum anti-back holding capability	300 lb.in.
Inertia, rotating parts	1.718 lb.in.^{2}
Maximum radial bearing load at maximum speed	63 lbs.
Maximum operating speed	500 RPM
Response time, voltage on at full speed	45 MS
Weight	7 lb.

b. MPB Commercial

Link to Data Sheet

magnetic particle BRAKE PLB-100 — 1.5 to 70 lb.-ft.

DATA SHEET

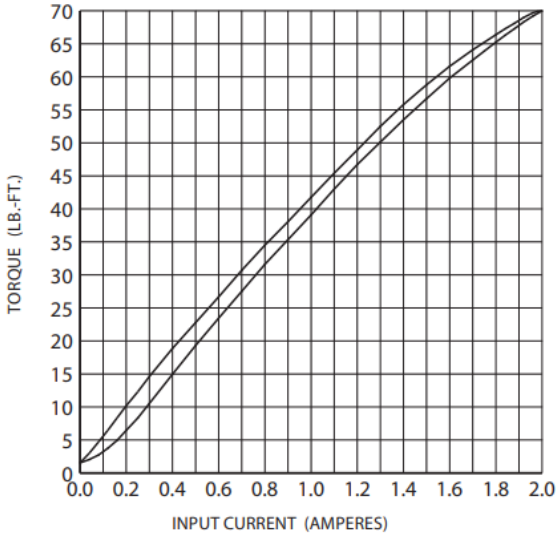

At brake temperature :	68°F	160°F
COIL RESISTANCE (ohms)	10.5	12.5
INPUT D.C. VOLTAGE, @ 2.0 amps	21	25

Do not exceed 2.0 amperes or 70 lb.-feet torque.

CHARACTERISTICS - With no electrical excitation, the shaft freely rotates. With electrical excitation, the shaft becomes coupled to the housing. Torque is proportional to input current (see torque graph), and independent of RPM. While the load torque is less than the output torque, the shaft won't rotate. When the load torque is increased, the brake will slip smoothly at the torque level set by the coil input current.

Torque range	1.5 to 70	lb.-ft.
De-magnetized drag torque	0.3	lb.-ft.
Maximum RPM	500	RPM
Heat dissipation	200	Watts
Heat dissipation, w/ piped air	300	Watts
Piped air pressure	7	psi
Piped air volume	8	$ft.^3$/minute
Maximum case temperature	160	degrees F
Maximum overhung load	175	lbs.
Shaft inertia	0.26	lb.-in.-sec ^{2}
Weight	30.5	lbs.

TORQUE CURVE - Use the lower torque curve when an input current value is approached from 0 amperes. Use the upper torque curve when the input current value is approached from the 100% input current.

Mount horizontally only.

BRAKE PERFORMANCE

TORQUE: At 20 volts, the brake will draw 100% of the rated input current, at 68°F. Output torque will be 70 lb.-ft.

POWER SUPPLY: A "constant-current" D.C. power supply is recommended for the best accuracy in open-loop control systems.

HEAT DISSIPATION: For continuous slip, calculate the heat input by the formula :

HEAT (watts) = RPM x TORQUE (lb.-ft.) x 0.14

Using the above formula: At rated torque, the maximum continuous RPM is 20, (31 with compressed air). The brake can dissipate higher amounts of heat for short periods of time, but the average must not exceed ratings. The case temperature must never exceed 160 degrees F.

INSTALLATION INFORMATION

Do not drop, or strike with a hammer. Keep away from fine metal filings and fine metal chips. Shield from liquids.

Do not attempt to remove the brake shaft or retaining ring.

All pulleys, sprockets, couplings, etc. must mount as slide fits. Use a puller to remove stuck components. Never pry or hammer to install or remove components.

Always use a flexible coupling when connecting the shaft of a rigidly mounted brake to the shaft of another rigidly mounted device. Precisely align both shafts.

Always electrically ground the brake.

COMPRESSED AIR COOLING For additional cooling, connect low pressure (7 psi max.) compressed air to the 1/4-19 BSPT tapped hole. (British Standard Tapered Pipe Thread). An adaptor fitting to 1/4" hose is included. Use clean, filtered, oil free, moisture free air.

PLACID INDUSTRIES Magnetic Particle Brakes & Clutches Hysteresis Brakes & Controls

1580 Lake Street • Elmira, NY 14901 • USA
518-523-2422 • 866-523-2423 • Fax: 518-523-2746 • placidindustries.com

c. Ratchet

120XP Ratchets

The Double-Pawl design of GEARWRENCH 120XP™ Ratchets provides 120 ratcheting positions so fasteners can be turned in the tightest spaces and jobs can be completed faster. Two pawls alternately engage a 60-tooth gear, allowing a swing arc of just 3 degrees and delivering strength that exceeds ASME torque performance requirements.

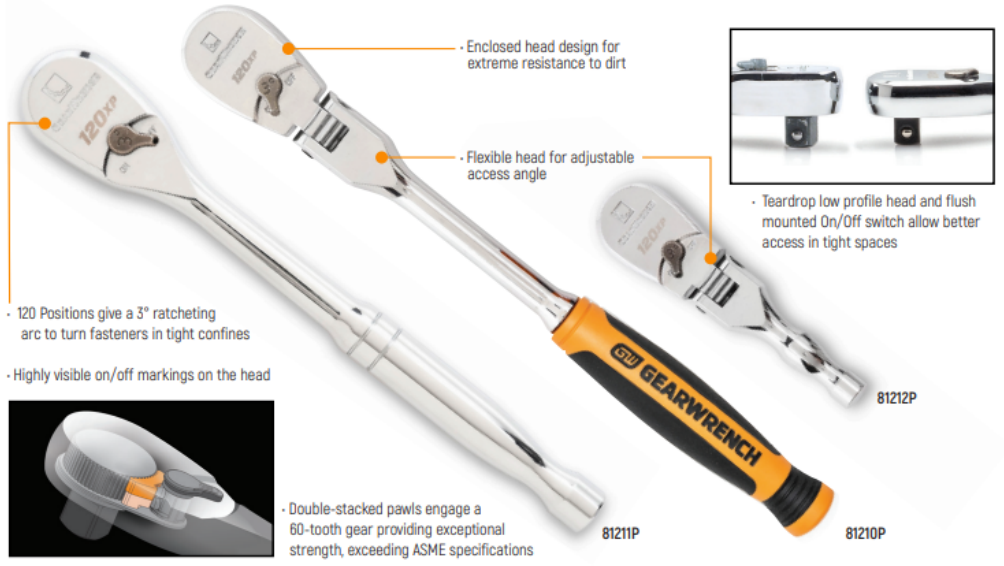

· Teardrop low profile head and flush mounted On/Off switch allow better access in tight spaces

SKU #	Drive Size	Head Style	Handle Style	Finish	Head Width	Head Thickness	Overall Length	Weight	Repair Kit
81011P	1/4"	Tear Drop	Standard	Full Polish	0.98	0.39	5.12	0.29	81099P
81034	1/4"	Tear Drop	Extra Long	Full Polish	0.98	0.39	9.00	0.77	81099P
81012P	1/4"	Tear Drop	Flex	Full Polish	1.02	0.41	6.85	0.33	81099P
81009P	1/4"	Tear Drop	Flex	Cushion Grip	1.02	0.41	8.18	0.36	81099P
81211P	3/8"	Tear Drop	Standard	Full Polish	1.25	0.55	8.38	0.72	81227P
81269	3/8"	Tear Drop	Extra Long	Full Polish	1.25	0.55	18.00	1.08	81227P
81215P	3/8"	Tear Drop	Flex	Full Polish	1.30	0.55	11.47	0.95	81227P
81212P	3/8"	Tear Drop	Stubby Flex	Full Polish	1.30	0.55	5.00	0.55	81227P
81210P	3/8"	Tear Drop	Flex	Cushion Grip	1.30	0.55	13.58	0.99	81227P
81304P	1/2"	Tear Drop	Standard	Full Polish	1.72	0.75	11.02	1.87	81339P
81364	1/2"	Tear Drop	Extra Long	Full Polish	1.72	0.75	24.00	2.86	81339P
81306P	1/2"	Tear Drop	Flex	Full Polish	1.72	0.75	16.90	2.44	81339P

C. Brake Holding Torque Calculations

a. Custom Wrap Spring Brake

Torque Requirement:
Bench tests on the analyzed custom wrap springs were conducted in a previous paper [53]:

3.1 Engineering Bench Tests

3.1.1 Wrap Spring Torque Tests

Objective

The hip and knee joints were tested to ensure they could hold at least 31 Nm of torque.

Methods

The test involved hanging weights off a moment arm connected to the joint and increasing the weights to see if the joints failed at a torque of 31 Nm. The moment arm was 6.8 cm at the knee and 7.4 cm at the hip. While loading the joint, the change in angle at the joint was recorded using a goniometer to measure the wrap spring slip. For example, first the joint was loaded with 1 kg and the angle was measured, then the load was increased to 5.7 kg and the angle was measured again. Each plot marker in Figure 3.2 indicates the torque due to load that at instant and the change in angle relative to the starting state (angle of slip).

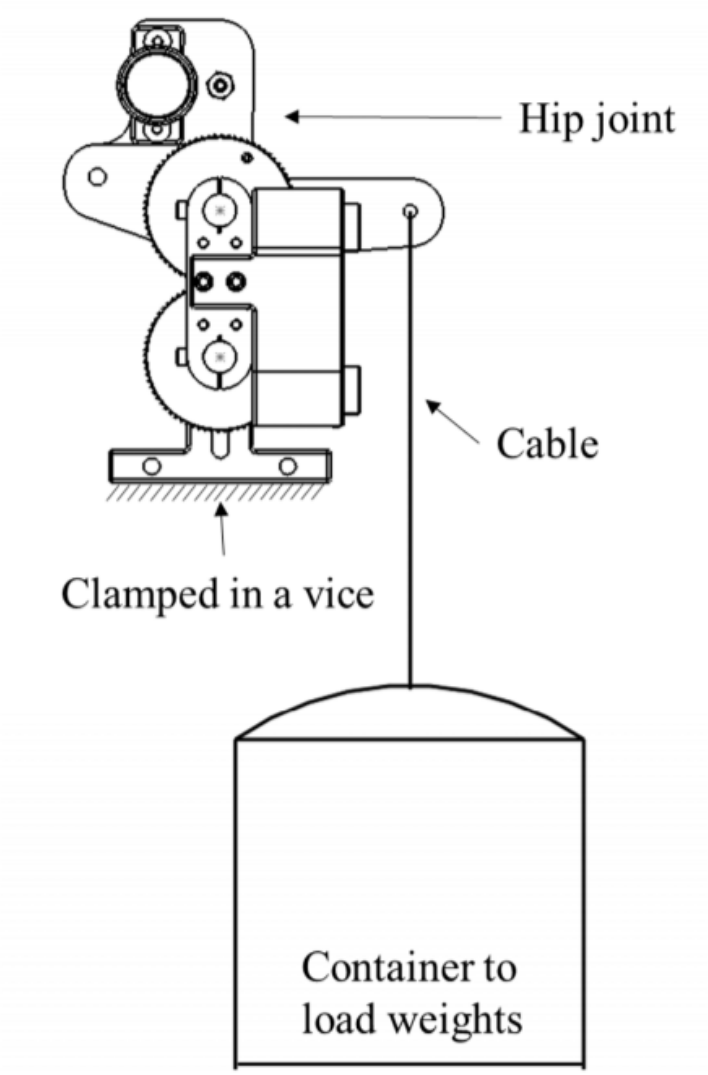

Figure 3.1: Hip joint wrap spring brake torque test

Results

The knee and the hip joints held a load of 50 Kg. This meant that the knee joint could hold at least 33.26 Nm and the hip joint could hold at least 36.17 Nm of torque. When the hip joint was loaded incrementally to around 53 kgs, the joint slipped by 8 deg (Figure 3.2).

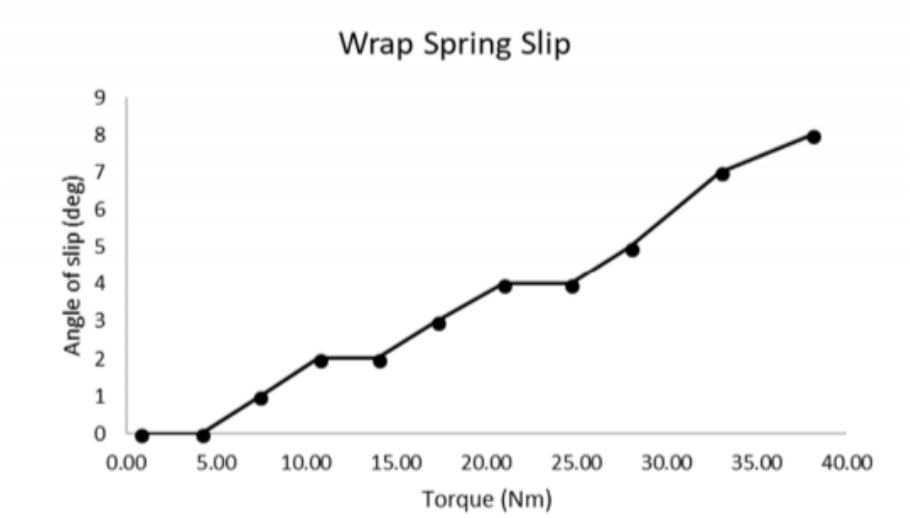

Figure 3.2: Wrap spring slip as the load varies

Discussion

The wrap spring brakes could hold the amount of torque required to prevent collapse of the user while standing. The slip of the wrap spring brake is its inherent characteristic. Each time the joint is loaded, the spring allows some movement before it coils down on the joint and stops the motion. This means that locking the joint at an exact angle is not possible with wrap spring brakes. However, to accomplish a gait cycle it is not necessary to accurately achieve the prescribed angles mentioned in Figure 2.2 which is why wrap spring brakes would work for this application.

b. Magnetic Particle Brake with a Transmission

Power Requirement:

An excerpt taken from a previous study on the magnetic particle brakes coupled with a transmission that was analyzed that provides data needed to calculate power requirement for each brake, "In steady state, when the hip brakes are resisting 1.8 Nm, they consume 350 mA at 10 V (3.5 W). When the knee brakes are resisting 2.8 Nm, they consume 350 mA at 28 V (9.8 W)" [28].

For the Hip Joint:

$$P = I \times V \text{ where } I = 0.35\,A \text{ and } V = 10\,V$$

$$\text{Therefore, } P = 3.5\,W$$

For the Knee Joint:

$$P = I \times V \text{ where } I = 0.35\,A \text{ and } V = 28\,V$$

$$\text{Therefore, } P = 9.8\,W$$

Torque Requirement:

The torque requirement for a magnetic particle brake with transmission was calculated by taking the continuous maximum torque provided by the manufacturer of the magnetic particle brake and multiplying it by the transmission ratio. Note that the manufacturer of the magnetic particle brakes used no longer exists and thus, the values have been taken from a previous paper in which these brakes were studied [28].

For the Hip Joint

Continuous maximum torque output is 1.8 N·m with a transmission ratio of 16:1
Therefore, the torque requirement is 28.8 N·m

For the Knee Joint

Continuous maximum torque output is 2.8 N·m with a transmission ratio of 16:1.
Therefore, the torque requirement is 44.8 N·m

D. Transmission Gear Selection

Gear Assumptions

- Custom made
- 0.125"=0.3175 cm face width for each gear
- 4140 Steel Alloy
- Gear in shape of cylinder for weight calculations with diameter as outside diameter of gear and length as face width
- Online gear weight calculator - https://www.onlinemetals.com/en/weight-calculator

Case 1: B15 MPB with a torque value of 1.69 Nm coupled with a 30:1 transmission (2000 max RPM)
Case 2: KB-5 MPB with a torque value of 51.52 Nm (1800 max RPM)
Case 3: B35 MPB with a torque value of 3.95 Nm coupled with a 13:1 transmission (1800 max RPM)

B15 MPB
Torque (MPB alone): 1.69 Nm
Weight (MPB alone): 1.13 kg
Transmission Ratio Needed for 50 Nm: 30:1

24 pitch:
Driven gear: Spur Gear - 24 pitch with 180 teeth (7.58"=19.25 cm outside diameter) (1.59 lbs = 0.72 kg weight divide by 6 since 60 deg range of motion --> 0.12 kg)
Driving gear: Spur Gear - 24 pitch with 6 teeth (0.33"=0.84 cm outside diameter) (0.003 lbs = 0.0014 kg weight)

Total Torque Value: 50.7 Nm
Total Weight = 1.13 kg (MPB) + 0.12 kg (driven gear) + 0.0014 (driving gear) = 1.2514 kg

18 pitch:
Driven gear: Spur Gear - 18 pitch with 180 teeth (10.11"=25.68 cm outside diameter) (2.82 lbs = 1.28 kg weight divide by 6 since 60 deg range of motion --> 0.21 kg)
Driving gear: Spur Gear - 24 pitch with 6 teeth (0.44"=1.12 cm outside diameter) (0.0053 lbs = 0.0024 kg weight)

Total Torque Value: 50.7 Nm

Total Weight = 1.13 kg (MPB) + 0.21 kg (driven gear) + 0.0024 (driving gear) = 1.3424 kg

KB-5 MPB
Torque (MPB alone): 51.52 Nm
Weight (MPB alone): 14.06 kg
No transmission needed

B35 MPB
Torque (MPB alone): 3.95 Nm
Weight (MPB alone): 1.81 kg
Transmission Ratio Needed for 50 Nm: 13:1

24 Pitch:
Driven gear: Spur Gear - 24 pitch with 130 teeth (5.5"=13.97 cm outside diameter) (0.837 lb = 0.38 kg weight divide by 6 since 60 deg range of motion --> 0.063 kg)
Driving gear: Spur Gear - 24 pitch with 10 teeth (0.5"=1.27 cm outside diameter) (0.0069 lb = 0.003 kg weight)

Total Torque: 51.25 Nm
Total Weight: 1.81 kg (MPB) + 0.063 kg (driven gear) + 0.003 kg (driving gear) = 1.876 kg

18 Pitch:
Driven gear: Spur Gear - 24 pitch with 130 teeth (7.33"=18.62 cm outside diameter) (1.49 lb = 0.68 kg weight divide by 6 since 60 deg range of motion --> 0.1133 kg)
Driving gear: Spur Gear - 24 pitch with 10 teeth (0.67"=1.70 cm outside diameter) (0.0124 lb = 0.006 kg weight)

Total Torque: 51.25 Nm
Total Weight: 1.81 kg (MPB) + 0.1133 kg (driven gear) + 0.006 kg (driving gear) = 1.9293 kg

E. Battery Calculations and Selection

To determine a capable battery for each of the analyzed brakes, the battery life in hours must be calculated using the below equation

Battery Life (in hours) = Battery Capacity (in Ah) / Load Current (in A)

Practical versions of a lower limb wearable robotic system need brakes with sufficiently low power requirements to enable an hour or more of use on a single battery charge. Thus, the battery life used in calculations will be one hour. The load current is the current of the magnetic particle brake being analyzed (Table E.1). The calculated battery life for each of the brakes using the above equation is included in the table.

Table E.1. Current, voltage, resistance, and power values and calculated battery life for each of the magnetic particle brake packages that were analyzed.

Brake	Current (A)	Voltage (V)	Resistance (Ω)	Power (W)	Battery Capacity (Ah)
MPB Commercial	2.0	21	10.5	42	2
MPB w/Transmission (Hip)	0.35	10	28.6	3.5	0.35
MPB w/Transmission (Knee)	0.35	28	80	9.8	0.35

Two batteries available commercially that have a lithium-ion battery chemistry with a battery capacity of 2 Ah and voltage of at least 21 V are shown below:

- Elecicopo 21V Lithium Ion Battery 2.0Ah Replacement Battery Compatible with Cordless Tools, Large Capacity Rechargeable Battery Pack for Cordless Power Tools Leaf Blower Electric Mini Chainsaw (Battery Only) → 360 grams Link
- **AOBEN 21V 2.0 Ah Li-ion Replacement Battery Compatible with AB7309 POWER Cordless Electric Drill → 351 grams Link**
    - Battery dimensions: 12.8 x 8.4 x 8.0 centimeters

A battery available from Digi-Key that has a lithium-ion battery chemistry with a battery capacity of 0.35 Ah and voltage of at least 10 V is shown below:

- **AUTEC Power Systems 18650 11.1 V Lithium-Ion Battery Rechargeable (Secondary) 2.3Ah APS28-LIR18650-2.3Ah → 180 grams Link**
    - Battery dimensions: 18.4 mm diameter and 64 mm length

Two batteries available from Digi-Key and Amazon that has a lithium-ion battery chemistry with a battery capacity of 0.35 Ah and voltage of at least 28 V is shown below:

- VARTA 51.8 V Lithium-Ion Battery Rechargeable (Secondary) 29Ah → 9600 grams Link
- LabTEC M28 28V 6000mAh Lithium Battery Replacement for Milwaukee 28V Battery M28 48-11-2830 48-11-2830 0726-22 0780-20 M28 0721-21 Cordless Power Tool → 721 grams Link
- **EMBRACESUN 3000mAh Battery Pack MIL28A Li-ion Battery 28V Replacement for Milwauk 28V Battery M28 V28 48-11-2830 with LED Gauge → 648 grams Link**
    - Battery dimensions: 13.2 x 8.4 x 6.2 centimeters

The batteries selected for use in analysis were selected because they provided sufficient battery capacity and voltage for the analyzed magnetic particle brakes while providing the least amount of weight compared to the other options. The selected batteries have been bolded.